

Anonymous Referee #1

General comments: This is a nice paper on using numerical modeling to address some important issues related to urban effects on the atmosphere. The paper is well written as a whole and easy to follow. The main idea is to analyze the relative importance of anthropogenic heat contribution to atmospheric patterns and its consequent effects on air pollution dispersion. Although the contribution seems to be small compared to other effects, it is clear that it is very important to correctly consider the AH sources during simulations, especially over very large urban areas. I consider the paper suitable for publication, after the verification of some small features, as listed in the specific comments below.

Thanks for the constructive and the affirmative comments.

Specific Comments and technical corrections:

Abstract: insert the acronym for boundary layer height before using it (see lines 23 and 26).

Thanks for the constructive comment. In the new revised manuscript, the acronym 'PBLH' is inserted after the words 'planetary boundary layer height' on line 26.

Page 2, lines 49-50 (and 201). Indicate which reference correspond to Zhang et al 2009. There are two different references with the same year.

Yes, there are two different references with the same year for 'Zhang et al., 2009' in the original manuscript. In the new revised manuscript, they are cited as 'Zhang et al., 2009a' and 'Zhang et al., 2009b', respectively. 'Zhang et al., 2009' on lines 49-50 of the original manuscript is changed to 'Zhang et al., 2009a' in the revised manuscript (lines 48-49). 'Zhang et al., 2009a' is written by Zhang D. L. et al. in 2009, which is listed on lines 887-888 in References of the revised manuscript. 'Zhang et al., 2009' on line 201 of the original manuscript is changed to 'Zhang et al., 2009b' in the revised manuscript (lines 205-206). This paper is written by Zhang Q. et al. in 2009, which is listed on lines 889-891 in References of the revised manuscript.

Page 5, line 172-173, the authors mention that the model domain has a resolution of 27 km x 27 km. Actually, this refers to the grid spacing, as you mention on line 175. Resolution has another meaning and it is related to the feature that you are able to represent in the model.

Thanks for the constructive comment. The words 'with the grid resolution of 27km × 27km' on lines 172-173 of the original manuscript are replaced by the words 'with the grid spacing of 27km'. Please see line 179 in the new revised manuscript.

The resolution of Fig 1 is to low. It would be better if the authors could improve it.

Thanks for the constructive comment. Fig. 1 is replaced by a new high quality figure, with the improved resolution of 600 dpi. Please see lines 212-217 in the new revised manuscript.

Page 6, lines 190-191. In the same way, the sentence “the resolution of 30-sec” should be changed by “30 arc seconds grid spacing”. Please, consider the same issue on lines 199 and 204. According to the suggestion, the sentence “the resolution of 30-sec” on lines 190-191 of the original manuscript is changed to “30 arc seconds grid spacing”, the words "with 0.25°× 0.25° resolution" on line 199 of the original manuscript is revised to "with 0.25° grid spacing", and the words "with the spatial resolution of 1°× 1°" on line 204 of the original manuscript is replaced by "with the grid spacing of 1°". Please see lines 194-195, lines 203-204, and line 208 in the new revised manuscript.

Page 8, lines 263-264 (and 278) the authors cited the reference Chen et al 2012a. However, there is just one reference by Chen et al in 2012, as you can see in the reference list. Sorry for this clerical mistake. The references cited on lines 263-264 of the original manuscript ("Chen et al. (2012; 2014a)") should be "Chen et al. (2012; 2014a)". We change the relevant words, and revise the related label of the papers in the reference list as well. Please see lines 276-277, and lines 751-755 of the new revised manuscript.

Page 8, line 266. Correct the figure number. The correct is 2f, instead of 4f. In the comparisons of Grd_AH against Fix_AH it would be useful for the readers to have a special view of the Fix_AH contributions. The values are fixed, but they certainly are heterogeneous around the domain. A figure similar to Fig. 2 would be nice. Sorry for this clerical mistake. The figure number "4f" on line 266 of the original manuscript is replaced by "2f". Please see line 279 of the new revised manuscript.

We agree that "the comparisons of Grd_AH against Fix_AH would be useful for the readers to have a special view of the Fix_AH contributions". So, Fig. 1b that is similar to Fig. 2 and some words are added to illustrate and compare the heterogeneity of AH distribution in Grd_AH and Fix_AH. Please see lines 212-217 and lines 288-295.

In page 16, section 3.3.3. The authors mention that the air near to the surface becomes dryer. It should be considered that the regions where RH is lower correspond mostly to the regions where temperature is higher. Therefore, it does not necessarily mean that the air is actually drier. I believe that this whole paragraph should be better explained. We agree that "the regions where RH is lower mostly correspond to the regions where temperature is higher", and RH is not the appropriate factor to explain whether the surface becomes dryer. So, in the new revised manuscript, we use the changes of water vapor mixing ratio at 2m between Grd_AH and Non_AH (Grd_AH minus Non_AH) to explain the effect of AH on surface moisture. We believe that the new figures (Fig. 6a and b) and new paragraph (lines 465-470) in the revised manuscript can better illustrate the phenomenon that the air near the surface becomes dryer.

Page 19, line 503. The correct statement is “atmospheric conditions” instead of “meteorology conditions”.

According to the suggestion, the words "meteorology conditions" in "Since adding AH changes the meteorology conditions" on line 503 of the original manuscript are changed to "atmospheric conditions". Please see line 534 of the new revised manuscript.

Page 25, line 652. The authors said that “. . . strong upward air flower. . .” Is that right?

Sorry for this clerical mistake. The words "strong upward air flower" on line 652 of the original manuscript are revised to "strong upward air flow". Please see line 683 of the new revised manuscript.

References:

Indicate in the list which references corresponds to Chen et al 2014 a and b. The same for Liu et al 2013 a and b, Wang et al 2009 a and b.

Two different references for ‘Chen et al., 2014’ are indicated as "Chen et al., 2014a" for the paper written by Chen, B., Dong, L., Shi, G. Y., et al. and "Chen et al., 2014b" for the paper written by Chen, B., Yang, S., Xu, X. D., et al., respectively. Please see lines 751-755 of the new revised manuscript. Meanwhile, the words "Chen et al., 2012a; 2014" on line 278 of the original manuscript are changed to "Chen et al., 2012; 2014a". Please see line 289 of the new revised manuscript.

Two different references for "Liu et al., 2013" are indicated as "Liu et al., 2013a" for the paper written by Liu, M., et al. and "Liu et al., 2013b" for the paper written by Liu, Q., et al., respectively. Please see lines 813-818 of the new revised manuscript. Meanwhile, the words "Liu et al., 2013" on line 164 of the original manuscript are revised to "Liu et al., 2013b" on line 171 of the new revised manuscript. The words "Following the work of Liu et al. (2013)" are replaced by "Following the work of Liu et al. (2013b)" on line 190 of the new revised manuscript.

Two different references for "Wang et al., 2009" are indicated as "Wang et al., 2009a" for the paper written by Wang T., et al. and "Wang et al., 2009b" for the paper written by Wang X. M., et al., respectively. Please see lines 861-866 of the new revised manuscript.

Word Bank Group, 2015, cited on page 3, is not correctly cited in the reference list.

In the reference list of revised manuscript, the cited document is corrected as "World Bank Group: East Asia's changing urban landscape: measuring a decade of spatial growth, World Bank, Washington Dc, 2015.". Please see lines 870-871 of the new revised manuscript.

Anonymous Referee #2

The article analyses the impacts of anthropogenic heat (AH) emissions on the atmospheric

conditions and air quality in South China considering January and July from 2014. The article is based in a spatial and temporal analysis of AH emissions from top-down energy inventory method and WRF/CHEM model simulations. This paper is very well written, organized, with very clear graphics/figures and with interesting analysis results. Despite of the positive view of the article, there are some deficiencies, but this referee recommends the manuscript to be accepted for publication in the Atmospheric Chemistry and Physics after suggested revisions are made. The suggestions are described below:

Thanks for the constructive and the affirmative comments.

Page 3, lines 84-86. The article showed that the main impacts of AH emissions were observed in Pearl River Delta (PRD) region. However, it is not presented an explanation of that region, such as which cities are located in that area. Please, for readers who do not know that area, provide more detailed information of the area, such as a map illustrating the location. In the same way, the article has a deficiency in the description of the South China region. This referee thinks that is important to describe some information about land use, land cover, topography, as well as the typical climatological and atmospheric conditions such as circulations breezes, among others.

Thanks for the constructive comment. To provide more detailed information of South China and PRD, Fig. 1b (with the green square to show the location of PRD) and some words (to briefly describe the information of topography, land use, climate, and atmospheric conditions, etc.) are added in the new revised manuscript. Please see lines 79-93 (brief description) and lines 212 -217 (Fig. 1b) in the revised manuscript.

Page 5, Figure 1 - The resolution of Figure 1 is not good. If possible, the authors could improve the figure.

Thanks for the constructive comment. Fig. 1 is replaced by a new high quality figure, with the improved resolution of 600 dpi. Please see lines 212-217 in the new revised manuscript.

Page 5, lines 176 - 178. In the description of chosen period, that is, January and July from 2014, the paper mentioned that "January and July are used to represent the hot and the cold weather condition, respectively", but the months of January and July represent the cold and hot months for the region analyzed, respectively. Also in this context, why did you choose those periods? Moreover, the use of monthly average could produce erroneous or masked results, since it includes days with different synoptic conditions.

Sorry for the clerical mistake "January and July are used to represent the hot and the cold weather condition, respectively". These words are changed to "In South China, January is generally representative of the relatively cold and dry season, while July represents the relatively hot and wet weather condition" in the new revised manuscript. Please see lines 183-186.

In the paper for studying the influence of urban expansion on O₃ distribution over the PRD region (Wang X. M. et al., 2014), it is reported that "Representations of seasonal results are created using hourly URB results from January and July. The two months are representative of the relatively

cold and dry season of the year, and the relatively hot and wet season of the year, respectively. ". So, we choose January and July of 2014 for our simulations. To better clarify our consideration, we rewrite the relevant sentences and cite the paper by Wang et al. (2014) in the new revised manuscript. Please see lines 183-186 and lines 867-869.

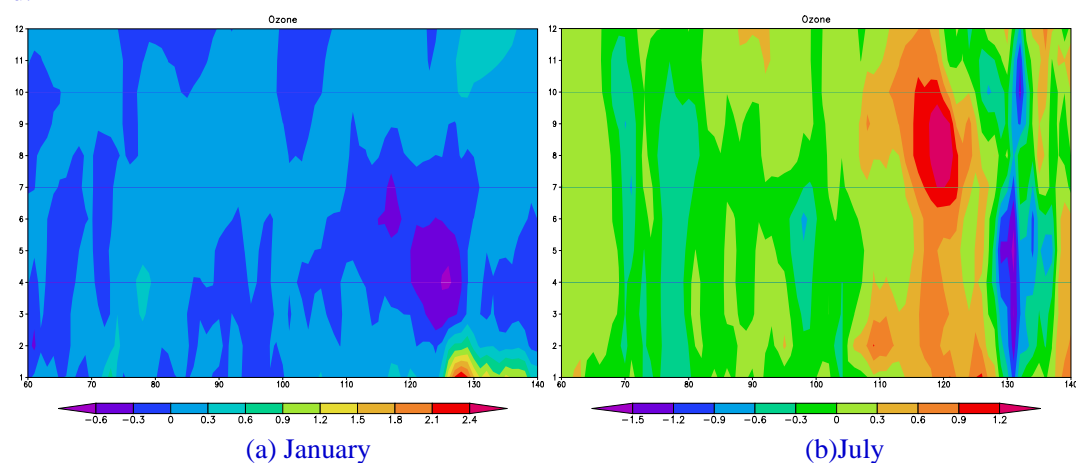
In previous studies, Ryu et al. (2013) studied the effects of AH based on an episode, while Yu et al. (2014) investigated this issue by using the monthly average (August) as well. We agree that "the use of monthly average could produce erroneous or masked results, since it includes days with different synoptic conditions.". But the main purpose of this paper is not to discuss the effect of AH on a pollution episode. We want to know the relative longtime effect of AH, its tendency, and the seasonal difference. In this case, it is a common method to use the monthly mean values to discuss the effect (Wang et al., 2014; Yu et al., 2014; Liao et al., 2015; Xie et al., 2016).

Page 6, lines 182-183. The authors present a vertical cross section analysis through the line AB reaching the Haikou and Guangzhou areas. However, it is not presented the motivation of choosing that line. If line AB was a latitudinal section, approximately 22.5°N or 23°N reaching the Nanning and Guangzhou areas, do you think it would be possible to find a different pattern from the impact of AH emissions? Why?

The vertical cross section analysis through the line AB is to discuss the different effects of AH on ambient environment between the big (Guangzhou) and the relatively small (Haikou) city. To better present the motivation of choosing this line, we add these words for explanation on lines 380-381 of the new revised manuscript.

We choose Haikou as the representative of relatively small cities because there are no other cities between Guangzhou and Haikou along line AB.

The AH emission in Haikou is close to that in Nanning. So, we believe that the vertical changing pattern from the impact of AH should be similar if line AB reaches Nanning and Guangzhou. We also do the vertical cross section analysis through the line reaching the Guangzhou and Nanning areas. The results are similar. For example, the following figures illustrate the vertical changes of O₃ impacted by adding AH (Grd_AH minus Non_AH). Obviously, they are similar to Fig. 9c and d.



Page 6, lines 186-193. In the description of the physical parameterizations schemes, it was mentioned about which urban canopy parameters were adopted. Then, it would be interesting to add a descriptive table that contains main urban parameters such as height of buildings and constructions, street and avenues information, albedo of urban areas, among others.

Thanks for the constructive comments. We add the descriptive table (Table 2) that contains the modified values of main urban parameters. Please see line 221 of the new revised manuscript. Additionally, we also add some explanation words for the table on lines 190-193.

Page 8, line 266. The mentioned figure seems to be wrong (Fig.4f). It would not be Fig.2f?

Sorry for this clerical mistake. The figure number "4f" on line 266 of the original manuscript is replaced by "2f". Please see line 279 of the new revised manuscript.

Page 12, line 358-360. The article demonstrates the impact of AH emissions on the atmospheric condition through the analysis of some variables such as wind speed at 10m (WS_{10}) and vertical wind velocity (w). Do you think that AH emissions can disturb the horizontal wind regime? How AH emissions can affect the land and the sea breezes circulation? The spatial and temporal patterns of these variables and their correlations would be investigated more properly.

We agree that AH emissions may affect the land and the sea breeze circulation. We also think that it is a good idea to study the influence of AH on these local breezes. We add "It is worth mentioning that the changes of vertical air movement and surface wind may affect the local land-sea breeze circulation in the coastal cities. For example, AH emission in Haikou enhances the upward air movement above the city (Fig. 6c and d), causes the downward movement above the surrounding waters (Fig. 6c and d), and increases the surface wind from sea to land (stronger convergence). These changes imply that AH might strengthen sea breeze in the daytime and weaken land breeze at night." in Section 3.3.2. We also add Fig. 7e and f to discuss the temporal pattern of the effect of AH on WS_{10} , and find that "For WS_{10} , AH emission causes it to increase 0.07 m/s in January and 0.15m/s in July. Most increases occur in the daytime. The effect of AH on surface wind is negligible at night, which may be related to the fact that the land breeze at night (from land to sea) hinders the surface convergence (from sea to land) caused by AH. ". Please see lines 458-463 and 520-524 in the new revised manuscript.

To perfectly discuss this issue, we should focus on a smaller region and use high-resolution simulations, which we plan to do in the future.

Page 13, line 381-382. The other deficiency is the description that AH emissions can modify the Urban Heat Islands (UHI). It appears to be questionable whether the increase in AH emissions can quantitatively enhance the UHI. The authors could provide concrete evidence of the UHI intensification. One way that authors can analyze could be the temperature difference between the most urbanized region (e.g. Guangzhou) and rural or less urbanized region (e.g. Nanning or Haikou) for simulations with (Grd_AH) and without adding AH (Non_AH). Therefore, perform an

analysis of the Urban Heat Island Intensity (or UHI) and examine whether results are in agreement with paper, so, if there is an intensification of the UHI when adding AH.

Thanks for the constructive comments. We perform an analysis of the Urban Heat Island Intensity, and find that AH emissions indeed enhance the UHI. For example, the UHI intensity (the difference of monthly mean temperature between the maximum in urban areas and the minimum in surrounding rural areas) in PRD is about 1.7°C in January and 1.3°C in July for Non_AH case, while it increases to 2.4°C in January and 1.8°C in July for Grd_AH case. These findings are added in the new revised manuscript. Please see lines 401-404.

Changes of regional meteorology induced by anthropogenic heat and their impacts on air quality in South China

Min Xie^{1,2,3*}, Kuanguang Zhu^{1,3,5}, Tijian Wang^{1,3,4*}, Wen Feng², ~~Minggao Li³~~, ~~Da Gao¹~~, Mengmeng Li¹, ~~Yong Han¹~~, Shu Li¹, Bingliang Zhuang^{1,3}, ~~Yong Han¹~~, ~~Pulong Chen¹~~, ~~Lei Shu¹~~, ~~Da Gao¹~~, Jingbiao Liao¹

¹ School of Atmospheric Sciences, Nanjing University, Nanjing, China;

² Key Laboratory of South China Sea Meteorological Disaster Prevention and Mitigation of Hainan Province, Haikou, China

³ [Jiangsu Collaborative Innovation Center for Climate Change, Nanjing, China;](#)

³ ~~[Hubei Academy of Environmental Science, Wuhan, China](#)~~

⁴ CMA-NJU Joint Laboratory for Climate Prediction Studies, Institute for Climate and Global Change Research, School of Atmospheric Sciences, Nanjing University, Nanjing, China;

⁵ [Hubei Academy of Environmental Science, Wuhan, China](#)

* [Correspondence to: Min Xie \(minxie@nju.edu.cn\)](mailto:minxie@nju.edu.cn) and [Tijian Wang \(tjwang@nju.edu.cn\)](mailto:tjwang@nju.edu.cn)

[Corresponding author, +86-25-89685302](mailto:minxie@nju.edu.cn)

[E-mail address: minxie@nju.edu.cn, tjwang@nju.edu.cn](mailto:minxie@nju.edu.cn)

Abstract: Anthropogenic heat (AH) emissions from human activities can change the urban circulation and thereby affect the air pollution in and around cities. Based on statistic data, the spatial distribution of AH flux in South China is estimated. With the aid of the WRF/Chem model in which the AH parameterization is developed to incorporate the gridded AH emissions with temporal variation, the simulations for January and July in 2014 are performed over South China. By analyzing the differences between the simulations with and without adding AH, the impact of AH on regional meteorology and air quality are quantified. The results show that the regional annual mean AH fluxes over South China are only 0.87W/m^2 , but the values for the urban areas of the Pearl River Delta (PRD) region can be close to 60W/m^2 . These AH emissions can significantly change the urban heat island and urban-breeze circulations in the big cities. In the PRD city cluster, 2-m air temperature rises up by 1.1°C in January and over 0.5°C in July, the [planetary](#) boundary layer height ([PBLH](#)) increases by 120m in January and 90m in July, 10-m wind speed is intensified over 0.35 m/s in January and 0.3 m/s in July, and the accumulative precipitation is enhanced by 20-40% in July. These changes of meteorological conditions can significantly impact the spatial and vertical distributions of air pollutants. Due to the increases of PBLH, surface wind speed and upward vertical movement, the concentrations of primary air pollutants decrease near surface and increase at the upper levels. But the vertical changes of O_3 concentrations show the different patterns in different seasons. The surface O_3 concentrations in

38 big cities increase with maximum values over 2.5ppb in January, while O₃ is reduced at the lower
39 layers and increases at the upper layers above some megacities in July. This phenomenon should
40 be attributed to the facts that the chemical effects can play a significant role in O₃ changes over
41 South China in winter, while the vertical movement can be the dominant effect in some big cities
42 in summer. Adding the gridded AH emissions can better describe the heterogeneous impacts of AH
43 on regional meteorology and air quality, suggesting that more studies on AH should be carried out
44 in the climate and air quality assessments.

45 **Key words:** Anthropogenic heat; PRD; WRF/Chem; PM₁₀; O₃

46
47 Urbanization and its impacts on regional meteorology and air quality have been widely
48 acknowledged, observed, and investigated (Rizwan et al., 2008; Mirzaei and Haghghat, 2010).
49 Previous studies have illustrated that urbanization can affect atmospheric environment in many
50 ways, which are mainly associated with the increase of air pollutant emissions from the
51 intensification of energy consumptions (Akbari et al., 2001; Civerolo et al., 2007; Jiang et al., 2008;
52 Stone, 2008; Chen et al., 2014b), the change of land covers from natural surfaces to artificial ones
53 (Civerolo et al., 2007; Lo et al., 2007; Wang et al., 2007; 2009b; Jiang et al., 2008; Zhang et al.,
54 | 2009a; Lu et al., 2010; Wu et al., 2011; Chen et al., 2014b; Liao et al., 2015; Zhu et al., 2015; Li et
55 al., 2016), and the release of anthropogenic heat from human activities in cities (Ryu et al., 2013;
56 Yu et al., 2014; Xie et al., 2016). Anthropogenic heat (AH) can increase turbulent fluxes in
57 sensible and latent heat (Oke, 1988), implying that it can modulates local and regional
58 meteorological processes (Ichinose et al., 1999; Block et al., 2004; Fan and Sailor, 2005; Ferguson
59 and Woodbury, 2007; Chen et al., 2009; Zhu et al., 2010; Feng et al., 2012; 2014; Menberg et al.,
60 2013; Ryu et al., 2013; Wu and Yang, 2013; Bohnenstengel et al., 2014; Chen et al., 2014a; Meng
61 et al., 2011; Yu et al., 2014; Xie et al., 2016) and thereby exert an important influence on the
62 formation and the distribution of ozone (Ryu et al., 2013; Yu et al., 2014; Xie et al., 2016) as well
63 as aerosols (Yu et al., 2014; Xie et al., 2016).

64 Previous studies on AH basically focused on the amount of heat fluxes or their effects on
65 meteorology. It was reported that the typical values of AH fluxes in urban areas range from 20 to
66 100 W/m² (Crutzen, 2004; Sailor and Lu, 2004; Fan and Sailor, 2005; Pigeon et al., 2007; Lee et
67 al., 2009; Iamarino et al., 2012; Lu et al., 2016; Xie et al., 2016). Sometimes, the fluxes might
68 exceed the value of 100 W/m² (Iamarino et al., 2012; Quah and Roth, 2012; Lu et al., 2016; Xie et
69 al., 2016), with the extreme value of 1590 W/m² in the densest part of Tokyo at the peak of
70 air-conditioning demand (Ichinose et al., 1999). In regard to their effects, the researchers found
71 that AH fluxes can cause urban air temperatures to increase by several degrees (Fan and Sailor,
72 2005; Ferguson and Woodbury, 2007; Chen et al., 2009; Zhu et al., 2010; Feng et al., 2012; 2014;
73 Menberg et al., 2013; Wu and Yang, 2013; Bohnenstengel et al., 2014; Chen et al., 2014a; Yu et al.,
74 2014; Xie et al., 2016), induce the atmosphere more turbulent and unstable, change the urban heat
75 island circulation, strengthen the air vertical movement (Ichinose et al., 1999; Block et al., 2004;

76 Fan and Sailor, 2005; Chen et al., 2009; Feng et al., 2012; 2014; Bohnenstengel et al., 2014; Yu et
77 al., 2014; Xie et al., 2016), enhance the convergence of water vapor in cities, and change the
78 regional precipitation patterns (Feng et al., 2012; 2014; Xie et al., 2016). In spite that meteorology
79 conditions and air quality are inextricably linked, however, few investigations have paid attention
80 to how the air quality is altered by the changes of regional meteorology induced by anthropogenic
81 heat. The results from the limited studies have showed that this impact is significant in and around
82 large urban areas and should be considered in the air pollution predictions (Ryu et al., 2013; Yu et
83 al., 2014; Xie et al., 2016).

84 Over the past decades, ~~many areas in~~ South China has been suffering the air quality
85 deterioration (Wang et al., 2007; 2009b; Chan and Yao, 2008; Liu et al., 2013b), with high ozone
86 (O₃) or poor visibility frequently occurring in urban areas (Wang et al., 2007; Fang et al., 2009)
87 and the background air pollutant concentrations steadily increasing (Wang et al., 2009a; Liu et al.,
88 2013b). South China generally refers to Guangdong, Guangxi, Hainan, Hong Kong, and Macau.
89 The main feature of the terrain is mountainous and hilly. The majority of South China has a humid
90 subtropical climate. Winters are mild, while summers are hot and muggy. It faces the South China
91 Sea to the south, and has the longest coastline in China. So there are many islands in South China,
92 including Hainan Island. These coastal areas can be influenced by both the monsoon and the
93 dreaded typhoon. These air pollutions in South China may be related with the rapid urban
94 expansion, especially in the Pearl River Delta (PRD) region. The PRD region consists of nine
95 cities in Guangdong Province (Guangzhou, Shenzhen, Zhuhai, Dongguan, Zhongshan, Foshan,
96 Jiangmen, Huizhou and Zhaoqing) plus Hong Kong and Macau (shown in the green square of Fig.
97 1b). As the most urbanized and industrialized part of South China, ~~the Pearl River Delta (PRD)~~
98 ~~region~~ has become the largest metropolitan area in the world within a very short time (Word Bank
99 Group, 2015). Thus, many previous studies have tried to figure out the effects of urbanization on
100 urban climate and air quality in this region (Lo et al., 2007; Wang et al., 2007; 2009b; Lu et al.,
101 2010; Meng et al., 2011; Wu et al., 2011; Zhang et al., 2011; Feng et al., 2012; 2014; Chen et al.,
102 2014b; Li et al., 2014; 2016). Among these studies, most researchers merely investigated how the
103 expansion of urban land-use influences the meteorology processes (Lo et al., 2007; Wang et al.,
104 2007; 2009b; Lu et al., 2010; Meng et al., 2011; Wu et al., 2011; Feng et al., 2012; Chen et al.
105 2014b; Li et al., 2016). Some also linked these changes of meteorological factors with the regional
106 air quality, and quantified the impacts of land-use changing on air pollution (Wang et al., 2007;
107 2009b; Feng et al., 2012; Chen et al., 2014b; Li et al., 2014; 2016). Only a few researchers took
108 AH into account (Meng et al., 2011; Feng et al., 2012; 2014). But they just clarified the impact of
109 AH on meteorological conditions by merely adopting the fixed AH value in the urban
110 parameterization scheme of meteorological models (Meng et al., 2011; Feng et al., 2012).
111 Consequently, we still need to further understand how the excessive anthropogenic heat from
112 urban expansion impacts on the severe air quality problems in this world famous region.

113 To fill the abovementioned knowledge gap, we present our new findings on the impact

114 mechanism of anthropogenic heat on urban climate and regional air quality over South China in
 115 this paper, including (1) the spatial and temporal characteristics of AH emissions in South China,
 116 (2) how to implement the inhomogeneous AH data into the air quality model WRF/Chem, (3) the
 117 impacts of AH fluxes on meteorological fields, and (4) the impacts of meteorology changes on the
 118 air quality in different cities over South China. Detailed descriptions about the estimating method
 119 for anthropogenic heat emissions, the adopted WRF/Chem model with special configurations, and
 120 the observation data for model validation are presented in Sect. 2. Main results, including the
 121 inhomogeneous distribution of AH, the model evaluation, and the three-dimensional changes of
 122 meteorological fields and air pollutant concentrations are presented in Sect. 3. The summary is
 123 given in Sect. 4.

124

125 **2. Methodology and data**

126 **2.1 Method for estimating anthropogenic heat fluxes**

127 The top-down energy inventory method, which predicts AH emissions based on the statistics
 128 data of energy consumption, is the most common approach and widely used all over the world
 129 (Sailor and Lu, 2004; Flanner, 2009; Hamilton et al., 2009; Lee et al., 2009; Allen et al., 2011;
 130 Iamarino et al., 2012; Quah and Roth, 2012; Chen et al., 2014a) as well as in China (Chen et al.,
 131 2012; Xie et al., 2015; 2016; Lu et al., 2016). On basis of the previous studies, AH fluxes over the
 132 area between (101°E, 16°N) and (119°E, 26°N) in 1990, 1995, 2000, 2005, 2010 and 2014 are
 133 calculated in this study by the following equation:

$$134 \quad Q_F = Q_{FI} + Q_{FB} + Q_{FV} + Q_{FHM} \quad (1)$$

135 where, Q_F is the total anthropogenic heat flux (W/m^2); Q_{FI} , Q_{FB} , Q_{FV} , and Q_{FHM} represent the heat
 136 emitted from the industry sector, buildings, vehicles and human metabolism (W/m^2), respectively.
 137 To accurate estimate the spatial heterogeneity of AH fluxes, the estimated area is gridded as 456
 138 rows and 264 columns with the grid spacing of 2.5 arcmin. The heat flux generated by human
 139 metabolism at each grid is estimated as:

$$140 \quad Q_{FHM} = P \cdot (M_d \cdot h_d + M_n \cdot h_n) / h \quad (2)$$

141 where, P is the population number at a grid. h_d , h_n and h are the hours of daytime, nighttime and a
 142 whole day. In this study, they are set to be 16, 8 and 24, respectively. M_d and M_n are the average
 143 human metabolic rate (W/person) during the daytime and at night. Referring to the previous
 144 studies (Sailor and Lu, 2004; Chen et al., 2012; Quah and Roth, 2012; Xie et al., 2015; 2016; Lu et
 145 al., 2016), we determined that the metabolic rate of a typical man is 175 W for the active daytime
 146 (M_d) and 75 W for the sleep period (M_n).

147 Based on the work of Flanner (2009), Lu et al. (2016) and Xie et al. (2016), it is reasonably
 148 assumed that all non-renewable primary energy consumption used for human activities is
 149 thermally dissipated as AH. So, Q_{FI} , Q_{FB} , and Q_{FV} at each grid can be estimated by using the data
 150 of non-renewable energy consumption (coal, petroleum, natural gas, and electricity etc.) from
 151 different categories. The amount of AH fluxes for one category can be estimated by the following

152 equation:

$$153 \quad Q_x = \eta \cdot \varepsilon \cdot C / (t \cdot A) \quad (3)$$

154 where, Q_x represents $Q_{E,I}$, $Q_{E,B}$ or $Q_{E,V}$. C is the primary energy consumption from a category at a
155 grid (metric ton standard coal). ε is the calorific value of standard coal equivalent, with the
156 recommended value of 29.271×10^3 kJ/kg (Chen et al., 2012; Lu et al., 2016; Xie et al., 2015;
157 2016). η is the efficiency of heat release, with the typical value of 60% for electricity or
158 heat-supply sector and 100% for other sectors (Lu et al., 2016; Xie et al., 2016). t is the time
159 duration of used data, which is set to be 31536000 s (seconds in a year) in this study. A represents
160 the area of a grid (km^2). To quantify the value of C for each grid, we first of all obtain the energy
161 consumption data from 1990 to 2014 in China Energy Statistical Yearbooks. Then we double
162 check and modify the data in typical cities on basis of the Yearbooks in Guangdong, Guangxi,
163 Hainan province and Hong Kong. In the end, the total numbers are apportioned according to the
164 value of gross domestic product (GDP) or population density at each grid. GDP is used for
165 industry and vehicle, while population is chosen for building. The population density with the
166 resolution of 2.5 arcmin in 1990, 1995, 2000, 2005 and 2010 can be downloaded from Columbia
167 University's Socioeconomic Data and Applications Center. The gridded GDP data are developed
168 and applied based on the work of Liu et al. (2013a). The spatial distributions of GDP and
169 population in 2014 are unobtainable, and thereby the data in 2010 are used as the surrogates.

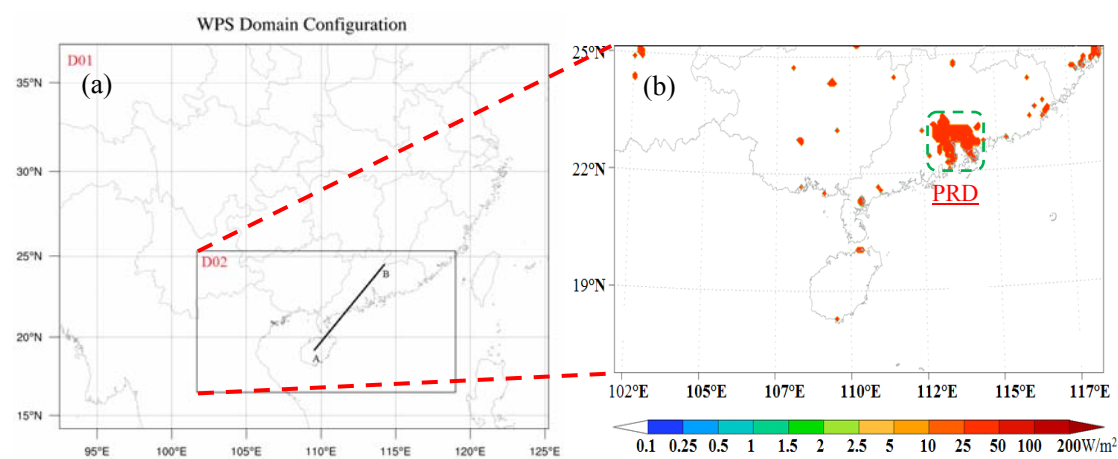
170 **2.2 WRF/Chem and its configuration**

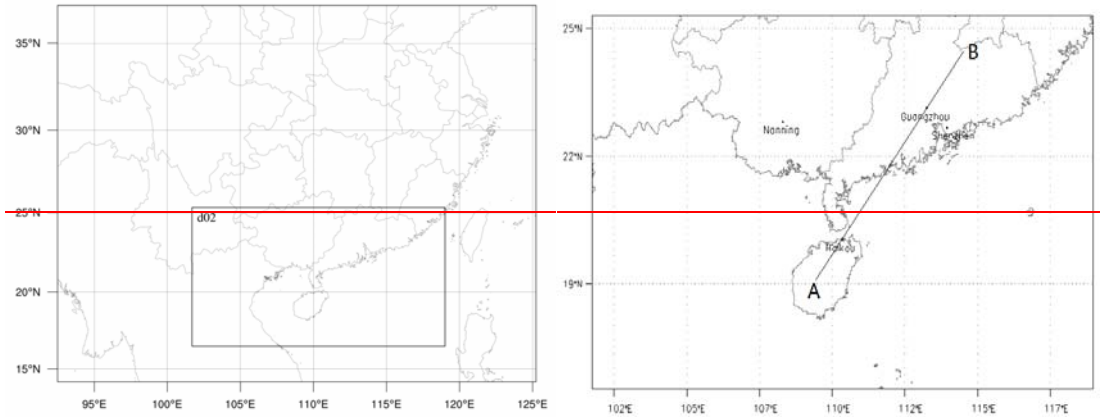
171 The WRF/Chem version 3.5 is applied to investigate the impacts of AH fluxes on regional
172 meteorology and air quality over South China. WRF/Chem is a new generation of air quality
173 modeling system, in which the feedbacks between meteorology and air pollutants are included by
174 fully coupling the meteorological model (WRF) with the chemical modules (Chem). WRF/Chem
175 has been widely used in simulating air quality in China and proved to be a reliable modeling tool
176 from city-scale to meso-scale (Wang et al., 2009b; Liu et al., 2013b; Yu et al., 2014; Liao et al.,
177 2015; Xie et al., 2016).

178 Three simulations are conducted in this study. One does not take the contribution of AH into
179 account while the other two incorporate WRF/Chem with the fixed or the inhomogeneous AH
180 fluxes (The details are presented in Sect. 2.3). Except for the setting of AH parameterization, other
181 configurations (such as the physical schemes, the chemical schemes and the emission inventories
182 etc.) for all simulations are the same. Thus, the difference between the modeling results can
183 illustrate the effects of AH. As shown in Fig. 1, two nested domains are used. The outermost
184 domain (Domain 1, D01) has the horizontal grids of 121×95 , with the grid ~~resolution-spacing~~
185 ~~27km~~ ~~×~~ ~~27km~~. The second domain (Domain 2, D02) covers Guangdong, Guangxi, and Hainan
186 provinces, with the center point at (110.4°E, 20.9°N), the horizontal grids of 192×105 , and the
187 grid spacing of 9km. For all domains, from the ground level to the top pressure of 100hPa, there
188 are 31 vertical sigma layers with about 10 in the planetary boundary layer (PBL). In South China,
189 January is generally representative of the relatively cold and dry season, while July represents the

190 relatively hot and wet weather condition (Wang et al., 2014). Thus, January and July ~~in of~~ 2014
191 are chosen for simulations and analysis in this study. ~~January and July are used to represent the hot~~
192 ~~and the cold weather condition, respectively.~~

193 The detailed options for the physical and chemical parameterization schemes used in this
194 study are shown in Table 1. Additionally, a Single Layer Urban Canopy Model (SLUCM) coupled
195 in Noah Land Surface Model (Noah/LSM) is adopted for better modeling the urban effects.
196 Following the work of Liu et al. (2013b) and Wang et al. (2014), the default values for urban
197 canopy parameters in SLUCM are substituted by the typical values in South China. As shown in
198 Table 2, the values for building height, roof width, road width, urban fraction, and surface albedo
199 are modified for the cities in and outside PRD, respectively. The recently updated Moderate
200 Resolution Imaging Spectroradiometer (MODIS) land-use data (20 categories) with ~~the resolution~~
201 ~~of 30- arc seconds grid spacing~~ are used to replace the default USGS (U.S. Geological Survey)
202 land-use data in WRF/Chem, because the USGS data are too outdated to illustrate the intensive
203 urbanization over South China. For chemistry, the RADM2 gas-phase chemistry scheme and the
204 MADE/SORGAM aerosol scheme are adopted. RADM2 (Regional Acid Deposition Model
205 version 2) contains 63 prognostic species and 136 reactions (Balzarini et al., 2015).
206 MADE/SORGAM is the classical aerosol module used in WRF/Chem (Grell et al., 2005), where
207 the Aerosol Dynamics Model for Europe (MADE) (Ackermann et al., 1998) contains the
208 Secondary Organic Aerosol Model (SORGAM) (Schell et al., 2001). The anthropogenic emissions
209 are mainly from the 2012-year Multi-resolution Emission Inventory for China (MEIC) with 0.25°
210 grid spacing × 0.25° resolution. This MEIC inventory based on RADM2 mechanism is re-projected
211 for the grids of China in both domains. For the grids outside of China, the inventory developed by
212 Zhang et al. (2009b) is used. The biomass burning emissions are acquired from the work of Li et
213 al. (2016). The biogenic emissions are calculated online by using MEGAN2.04 (Guenther et al.,
214 2006). The NCEP global reanalysis data with the ~~spatial resolution~~ grid spacing of 1° × 1° and 27
215 vertical levels are selected to provide the initial meteorological fields and boundary conditions.
216 The initial chemical state and boundary conditions are obtained from the modeling results from
217 the global chemistry transport model MOZART-4.





220
221 **Fig. 1. WRF/Chem domain configuration, including (a) two-way domains for simulations and (b) enlarged view**
222 **of domain 2 with fixed AH value of 50 W/m² for all urban grids used in the simulation case Fix_AH the cities**
223 **in South China where the observation sites are located. Line AB in (b) denotes the location of the vertical**
224 **cross section used in Fig. 4, Fig. 6, Fig. 8, Fig. 9, and Fig. 10. The green square in (b) presents the location of**
225 **the Pearl River Delta (PRD) region.**

226
227 **Table 1. The grid settings, physics and chemistry options for all simulations**

Items	Contents
Dimensions (x,y)	(121,95), (192,105)
Grid size (km)	27, 9
Time step (s)	150
Microphysics	Purdue Lin microphysics scheme (Lin et al., 1983)
Long-wave radiation	RRTM scheme (Mlawer et al., 1997)
Short-wave radiation	Goddard scheme (Kim and Wang, 2011)
Cumulus parameterization	Grell 3D (Grell and Devenyi, 2002)
Surface layer	Eta similarity (Janjic, 1994)
Land surface	Noah land surface model (Chen and Dudhia, 2001)
Planetary boundary layer	Mellor-Yamada-Janjic scheme (Janjic, 1994)
Gas-phase chemistry	RADM2 (Stockwell et al., 1990)
Photolysis scheme	Madronich photolysis (Madronich, 1987)
Aerosol module	MADE (Ackermann et al., 1998) / SORGAM (Schell et al., 2001)

228
229 **Table 2. The modified values of main urban canopy parameters for the PRD region and other cities.**

Parameter	Unit	PRD	Other cities
<u>Building height</u>	<u>m</u>	<u>20</u>	<u>10</u>
<u>Roof width</u>	<u>m</u>	<u>15</u>	<u>10</u>
<u>Road width</u>	<u>m</u>	<u>10</u>	<u>10</u>
<u>Urban fraction</u>	<u>Fraction</u>	<u>0.95</u>	<u>0.9</u>
<u>Surface albedo of roof</u>	<u>Fraction</u>	<u>0.2</u>	<u>0.2</u>
<u>Surface albedo of wall</u>	<u>Fraction</u>	<u>0.2</u>	<u>0.2</u>
<u>Surface albedo of road</u>	<u>Fraction</u>	<u>0.2</u>	<u>0.2</u>
<u>roughness length for momentum over roof</u>	<u>m</u>	<u>0.15</u>	<u>0.15</u>
<u>roughness length for momentum over wall</u>	<u>m</u>	<u>0.05</u>	<u>0.05</u>
<u>roughness length for momentum over road</u>	<u>m</u>	<u>0.05</u>	<u>0.05</u>

230
231 **2.3 The configurations for AH parameterization**

232 As shown in Table 23, three cases of numerical experiments are performed to evaluate the
233 effects of AH. Non_AH is the base case, which does not consider the effects of AH. In Fix_AH,
234 the default option for AH in SLUCM of WRF/Chem is adopted. For Grd_AH, we modify the AH
235 parameterization, and the gridded AH flux data estimated in Sect. 2.1 are used to simulation the
236 spatial heterogeneous effects of AH on meteorology and air quality. The difference between the

237 modeling results of Fix_AH and Grd_AH can illustrate the model improvement caused by
 238 considering the spatial heterogeneity of AH. Comparing the results from Non_AH and Grd_AH,
 239 we can finally demonstrate the exact impacts of anthropogenic heat.

240

241 **Table 2/ Table 3. Three simulations conducted in this study**

Cases	Description
Non_AH	excluding anthropogenic heat emissions in SLUCM
Fix_AH	including anthropogenic heat emissions in SLUCM, but using the default AH option with fixed value 50 W/m ² for all urban grids
Grd_AH	including anthropogenic heat emissions in SLUCM, and using the inhomogeneous AH emissions in 2014 estimated in Sect. 2.1

242

243 In SLUCM of WRF/Chem, the AH for one grid is determined by the fixed AH value, the
 244 fixed temporal diurnal pattern, and the urban fraction value (Chen et al., 2011; Yu et al., 2014; Xie
 245 et al., 2016). This default parameterization for AH can be described by the following algorithm:

$$246 \quad SH = F_V \cdot SH_V + F_U \cdot (SH_U + AH_{fixed}) \quad (4)$$

247 where SH is the total sensible heat flux in a grid. F_V and SH_V are the fractional coverage and the
 248 sensible heat flux of vegetations, respectively. F_U and SH_U are those of urban surfaces. AH_{fixed}
 249 represents the fixed AH value for all urban areas (Chen et al., 2011). With respect to Grd_AH, we
 250 modify Eq. 4 by incorporating the inhomogeneous AH data (Q_F) as follow:

$$251 \quad SH = F_V \cdot SH_V + F_U \cdot (SH_U + Q_F) \quad (5)$$

252 The gridded AH fluxes in 2014 from Sect. 2.1 (with the grid spacing of about 4km) are
 253 re-projected to domain 2 (9km) by the coordinates of each grid. To account for temporal variability,
 254 the diurnal variation pattern recommended for PRD by Zheng et al. (2009) and Lu et al. (2016) is
 255 adopted. It was reported that there is no significant seasonal difference in heating over South
 256 China (Lu et al., 2016). Thus, the monthly variation of AH is not considered in this study.

257 **2.4 Method for model evaluation**

258 The observation data of meteorology factors and air pollutants in Guangzhou, Shenzhen,
 259 Nanning and Haikou are used to validate the WRF/Chem simulations in this study. The hourly
 260 observation records of 2-m temperature, 10-m wind speed and 2-m relative humidity in January
 261 and July of 2014 can be obtained from the National Meteorological center of China
 262 Meteorological Administration. The relevant time series of PM₁₀ and O₃ concentrations can be
 263 acquired from China National Environmental Monitoring Center. The assurance/quality control
 264 (QA/QC) procedures for these data strictly follow the national standards. As described by Liao et
 265 al. (2015) and Xie et al. (2016), the mean bias (MB), root mean square error (RMSE) and
 266 correlation coefficient (COR) between observation records and modeling results are used to
 267 evaluate the model performance.

268

269 **3. Results and discussions**

270 **3.1 Spatial distribution of AH fluxes in South China**

271 Fig. 2 shows the spatial distribution of AH in 1990, 1995, 2000, 2005, 2010 and 2014 over

272 South China. Obviously, big cities especially the cities in PRD have the largest values from the
273 1990s till now. In 1990, except for those in Guangdong and Hong Kong, the AH fluxes in most
274 areas of South China are less than 2 W/m^2 . From 1995 to 2000, the AH fluxes in most parts of
275 PRD (except for those in Hong Kong) are less than 5 W/m^2 , and those in other areas of South
276 China are generally lower than 2.5 W/m^2 . After 2005, however, the AH fluxes exceed 10 W/m^2 in
277 many cities of South China, with the high values over 50 W/m^2 in and around Hong Kong. For the
278 annual mean AH flux over the whole administrative district of different province, the value in
279 Guangdong continuously increases from 0.30 W/m^2 for 1990 to 1.68 W/m^2 for 2014, while the
280 heat release in Guangxi and Hainan keeps in a low level ($< 0.5 \text{ W/m}^2$) but with an obvious
281 increasing. The annual mean AH values in the downtown areas are much higher than the regional
282 ones. For instance, the PRD city cluster always has the highest anthropogenic heat emissions in
283 South China. As shown in ~~Table 3~~ Table 4, the annual mean value in the built-up areas aggrandizes
284 from 5.1 W/m^2 in 1990 to 58 W/m^2 in 2014. These results are similar to those reported by Chen et
285 al. (2012a; 2014a) and Xie et al. (2015), and the temporal variation pattern also fits in well with
286 the economic boom over South China in the past decades.

287 In 2014, as illustrated in Fig. ~~4f~~ 2f, most important cities in South China have the AH fluxes
288 more than 5 W/m^2 . High fluxes generally occur in Guangdong province, especially in the PRD
289 region and the Chao-Shan area, with the typical values over 10 W/m^2 . In the build-up area of
290 Guangzhou, the AH fluxes are close to 60 W/m^2 , which are similar to those in Seoul of Korea (Lee
291 et al., 2009), Toulouse of France (Pigeon et al., 2007), and some US cities (Sailor and Lu, 2004;
292 Fan and Sailor, 2005). The regional highest value occurs in Hong Kong, with the value exceeding
293 100 W/m^2 . This value is comparable to those in the most crowded megacities, such as Shanghai
294 (Xie et al., 2016), Tokyo (Ichinose et al., 1999), London (Hamilton et al. 2009; Iamarino et al.
295 2012), and Singapore (Quah and Roth, 2012). In Nanning and Haikou, the annual mean AH fluxes
296 over the whole administrative district are close to 10 W/m^2 . These results can also be supported by
297 other previous investigations (Flanner, 2009; Chen et al., 2012; 2014a; Xie et al., 2015; Lu et al.,
298 2016). With regard to the default AH option in WRF/Chem, the fixed value of 50 W/m^2 is usually
299 used for all urban grids (shown in Fig. 1b). Compared with this unrealistic distribution pattern (Fig.
300 1b), ~~Our~~ our spatial distribution of AH based on the population (Fig. 2f) reflects the heterogeneity
301 of economic activities in South China, suggesting that our method is effective and the results are
302 reasonable. ~~These results can be supported by other previous investigations (Flanner, 2009; Chen~~
303 et al., 2012a; 2014; Xie et al., 2015; Lu et al., 2016). So, our AH data can be used in models to
304 investigate their impacts on urban climate and air quality.

305

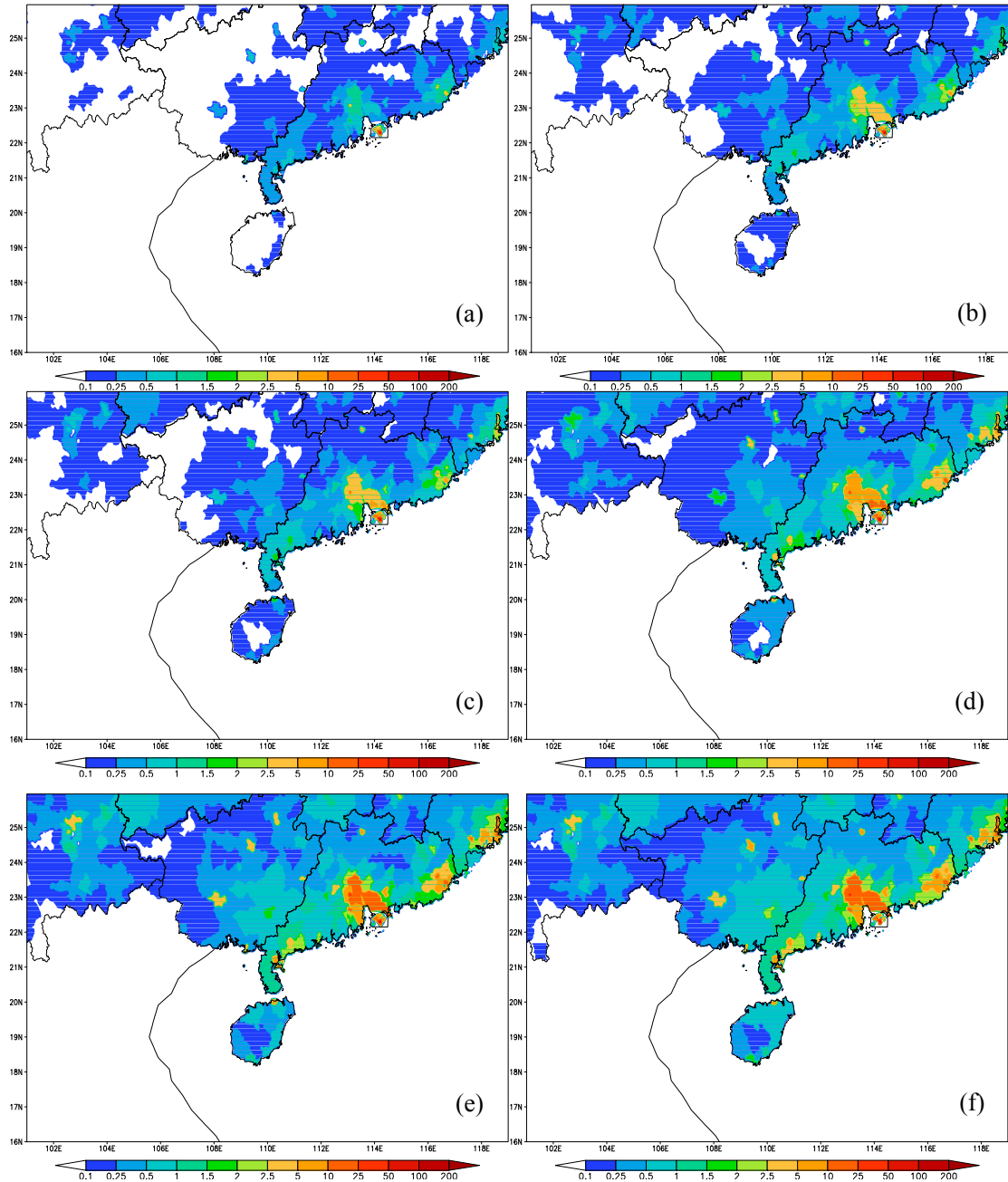


Fig. 2. Annual-mean anthropogenic heat fluxes between (101°E, 16°N) and (119°E, 26°N) with the resolution of 2.5 arcmin in 1990 (a), 1995 (b), 2000 (c), 2005 (d), 2010 (e) and 2014 (f), respectively.

Table 3 Table 4 Annual average anthropogenic heat flux in different administrative district over South China (W/m²)

Province		This study					
		1990	1995	2000	2005	2010	2014
Guangdong	Regional ^a	0.30	0.48	0.61	1.05	1.53	1.68
	Urban area in PRD	5.11	11.13	14.51	30.82	49.41	58.03
Guangxi	Regional ^a	0.11	0.16	0.17	0.26	0.38	0.44
Hainan	Regional ^a	0.04	0.09	0.14	0.23	0.37	0.49

^a Regional represents the average value over the whole area of a province

3.2 Simulation performance

317 To evaluate the model performance and clarify the better AH parameterization, the modeling
318 results from Fix_AH and Grd_AH are compared with the observation data in two typical months
319 (January and July). [Table 4Table 5](#) presents the performance statistics, including the values of
320 monthly mean (Mean), mean bias (MB), root mean squared error (RMSE) and correlative
321 coefficient (COR), which are all quantified for 2-m temperature (T_2), 2-m relative humidity (RH_2),
322 10-m wind speed (WS_{10}), ozone (O_3), and particles (PM_{10}) in Guangzhou (GZ), Shenzhen (SZ),
323 Nanning (NN), and Haikou (HK).

324 As shown in [Table 4Table 5](#), the correlation coefficients (COR) between observations and
325 simulations at four sites are generally about 0.80 for T_2 , over 0.75 for RH_2 , and close to 0.70 for
326 WS_{10} in both January and July (statistically significant at the 95 % confident level). So adding AH
327 in WRF/Chem (Fix_AH and Grd_AH) can well describe the urban meteorological conditions in
328 the typical cities over South China. Compared with the observation records of T_2 , except for
329 Shenzhen in January, both Fix_AH and Grd_AH tend to slightly simulate higher 2-m air
330 temperature at four sites in both months, which can be attributed to the uncertainty of urban
331 canopy and surface parameters (Liao et al., 2015; Xie et al., 2016). These overestimates are
332 acceptable because the MB values are smaller than 1.8 °C in January and smaller than 0.8 °C in
333 July. Moreover, when the gridded AH fluxes are taken into account (Grd_AH), the modeling
334 results of air temperature can be improved, with the mean bias (MB) decreasing by 0.1 - 0.3 °C
335 and the correlation coefficient (COR) increasing by 0.02 - 0.05 (from Fix_AH to Grd_AH). With
336 regards to RH_2 , the modeling values from two simulations (Fix_AH and Grd_AH) are close to the
337 observations. The best simulation occurs in Haikou, and the results at the other three sites are
338 reasonable as well, only with the bias within $\pm 10\%$. These 2-m relative humidity predictions can
339 be improved from Fix_AH to Grd_AH. When we consider the heterogeneity of AH fluxes in
340 Grd_AH, the values of MB and RMSE are closer to 0 and those of COR are closer to 1. For WS_{10} ,
341 because the modeling near-surface wind speed is generally influenced by local underlying surface
342 characteristics more than other meteorological parameters (Liao et al., 2015; Xie et al., 2016), both
343 Fix_AH and Grd_AH slightly overvalue the 10-m wind speed at four sites. In case Fix_AH, the
344 MB for WS_{10} is generally around 1m/s in both months, and the RMSE is less than 2.6 m/s in
345 January and around 2m/s in July. However, the predictions are obviously improved in case
346 Grd_AH. The MB decreases to 0.4-0.9 m/s in January and 0.4-0.7 m/s in July, and the values of
347 COR also increase from 0.68 (Fix_AH) to 0.74 (Grd_AH) in July. These improvements from
348 Fix_AH to Grd_AH for T_2 , RH_2 and WS_{10} predictions suggest that the default value of
349 WRF/Chem for all urban grids overestimates the AH fluxes in these cities, and our gridded AH
350 data as well as the new parameterization scheme can exactly catch the heterogeneity of the heat
351 released from the metropolitans of South China.

352 [Table 4Table 5](#) also illustrates the performance of WRF/Chem simulations for the main air
353 pollutants (O_3 and PM_{10}). Obviously, both Fix_AH and Grd_AH can capture the magnitude and
354 temporal variation of main air pollutants in these typical cities over South China, and the

355 simulation with gridded AH fluxes (Grd_AH) can provide better predictions. For Grd_AH, the
356 correlation coefficients (COR) for PM₁₀ in all cities are around 0.62 in January and around 0.65 in
357 July (statistically significant at the 95 % confident level). The MB values for PM₁₀ are only -0.4 -
358 1.0 µg/m³ in January and 1.8 -3.1 µg/m³ in July. With respect to O₃, the values of MB are -9.2 -
359 -16.1 ppb in January and -10.0 - -13.5 ppb in July. These underestimates should be related with the
360 increasing of WS₁₀ and the rising of PBL caused by positive biases in T₂. The uncertainties in
361 emissions of ozone precursors (NO_x and VOCs) may cause these biases as well (Liao et al., 2015;
362 Xie et al., 2016). However, the values of COR for O₃ are 0.60 - 0.71 in January and 0.60 - 0.64 in
363 July (statistically significant at the 95 % confident level), proving that these modeling results are
364 reasonable and acceptable.

365 Fig. 3 presents the monthly-averaged differences of O₃ and PM₁₀ between Fix_AH and
366 Grd_AH (Fix_AH minus Grd_AH) at the surface layer over the modeling domain 2 (D02).
367 Obviously, there are some differences between the two simulations that use different AH
368 parameterizations. These differences are more obvious in and around big cities because the AH are
369 related with the human activities. Moreover, the differences in January are higher than those in
370 July, implying that the adding of AH can arouse more atmospheric disturbances in winter. From
371 this point of view, Grd_AH can better describe the spatial and temporal heterogeneity of the
372 impacts of AH on regional air quality.

373 | **Table 4** **Table 5** Summary of statistics for comparison between simulated and observed hourly averaged meteorological and chemical data in four cities of South China

Case		Fix_AH										Grd_AH									
Vars ^a	Site _b	January					July					January					July				
		Mean ^c		MB	RMS E	COR _f	Mean ^c		MB	RMS E	COR _f	Mean ^c		MB	RMS E	COR _f	Mean ^c		MB	RMS E	COR _f
		SIM ^d	OBS ^e				SIM ^d	OBS ^e				SIM ^d	OBS ^e				SIM ^d	OBS ^e			
T ₂ (°C)	GZ	14.0	12.2	1.8	3.1	0.75	29.0	28.4	0.6	4.0	0.72	13.8	12.2	1.6	2.9	0.78	28.8	28.4	0.4	2.1	0.76
	HK	18.9	17.3	1.6	2.0	0.79	29.0	28.4	0.6	1.7	0.79	18.5	17.3	1.3	1.8	0.81	28.9	28.4	0.5	1.6	0.83
	NN	13.9	12.2	1.7	2.9	0.84	28.0	27.7	0.3	2.5	0.77	13.7	12.2	1.4	2.7	0.86	27.9	27.7	0.2	2.0	0.81
	SZ	14.6	14.7	-0.1	1.8	0.84	29.9	29.1	0.8	2.0	0.76	14.4	14.7	-0.3	1.9	0.86	29.6	29.1	0.5	1.9	0.81
RH ₂ (%)	GZ	64.2	73.5	-9.3	18.5	0.74	68.4	78.8	-10.4	17.9	0.73	66.8	73.5	-6.7	16.8	0.75	71.3	78.8	-7.5	16.8	0.76
	HK	75.6	78.2	-2.5	8.5	0.77	80.6	81.0	-0.3	7.8	0.80	77.0	78.2	-1.1	8.2	0.84	81.4	81.0	0.4	7.7	0.86
	NN	69.3	77.9	-8.6	18.2	0.74	87.7	83.5	4.2	8.8	0.79	72.3	77.9	-5.6	17.7	0.75	86.5	83.5	3.0	8.9	0.81
	SZ	65.9	63.3	2.6	11.7	0.75	74.2	78.0	-3.8	11.1	0.75	66.5	63.3	3.2	12.3	0.76	75.6	78.0	-2.4	10.5	0.83
WS ₁₀ (m/s)	GZ	3.1	2.4	0.7	1.9	0.75	2.6	1.8	0.8	1.8	0.68	2.8	2.4	0.4	1.3	0.76	2.4	1.8	0.6	1.4	0.74
	HK	4.3	3.3	1.0	2.3	0.74	3.6	2.7	0.9	1.7	0.68	4.2	3.3	0.9	1.8	0.76	3.2	2.7	0.5	1.4	0.74
	NN	2.5	1.3	1.2	2.3	0.73	2.3	1.5	0.8	2.1	0.68	2.0	1.3	0.7	1.5	0.75	1.9	1.5	0.4	1.2	0.74
	SZ	3.3	2.2	1.1	2.6	0.73	2.8	1.8	1.0	1.8	0.68	2.9	2.2	0.7	1.2	0.75	2.5	1.8	0.7	1.7	0.73
O ₃ (ppb)	GZ	93.7	110.5	-16.8	66.6	0.55	42.2	57.0	-14.8	62.5	0.51	101.3	110.5	-9.2	68.3	0.68	45.3	57.0	-11.7	52.5	0.64
	HK	63.7	75.5	-11.8	48.7	0.58	15.4	25.3	-9.9	25.8	0.51	65.4	75.5	-10.1	48.2	0.71	15.3	25.3	-10.0	21.7	0.63
	NN	138.4	157.8	-19.4	85.4	0.54	33.8	48.9	-15.1	55.4	0.51	141.7	157.8	-16.1	79.5	0.62	35.4	48.9	-13.5	48.6	0.60
	SZ	64.7	80.0	-15.3	54.2	0.52	28.7	43.9	-15.5	50.1	0.52	67.3	80.0	-12.7	56.5	0.60	31.6	43.9	-12.3	41.0	0.61
PM ₁₀ (µg/m ³)	GZ	21.1	19.6	1.5	13.0	0.53	31.4	28.9	2.5	29.0	0.53	20.3	19.6	0.7	12.2	0.61	31.0	28.9	2.1	25.3	0.63
	HK	32.2	30.9	1.3	14.5	0.53	14.7	11.9	2.8	15.3	0.53	31.9	30.9	1.0	14.1	0.61	14.2	11.9	2.3	13.9	0.63
	NN	25.6	24.7	0.9	16.7	0.54	19.8	17.3	2.5	12.7	0.54	25.3	24.7	0.6	15.7	0.62	19.1	17.3	1.8	9.0	0.65
	SZ	27.7	28.4	-0.7	14.3	0.54	24.5	20.6	3.9	17.8	0.55	28.0	28.4	-0.4	13.4	0.62	23.7	20.6	3.1	14.3	0.66

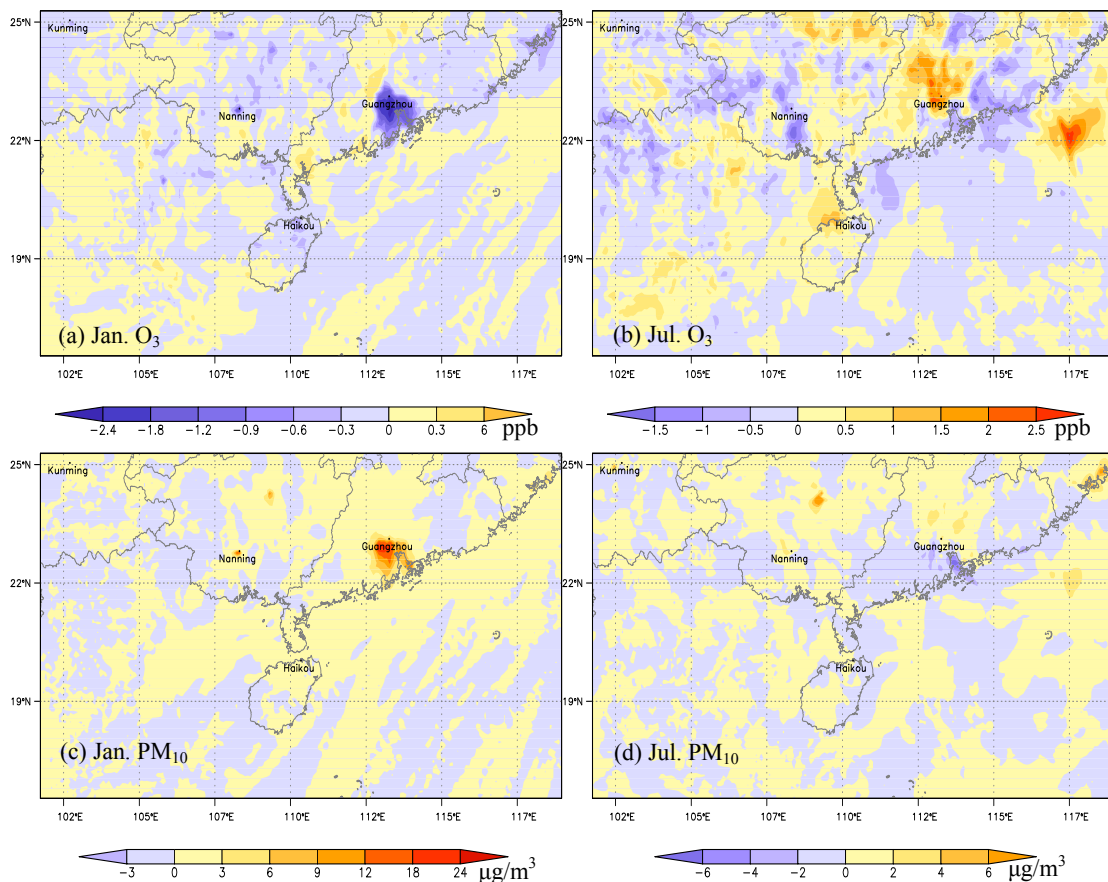
374 ^a Vars indicates the variables, including temperature at 2m (T₂), relative humidity at 2m (RH₂), wind speed at 10m (WS₁₀), ozone (O₃) and PM₁₀; ^b Site indicates the city where the observation
375 sites locate, including Guangzhou (GZ), Haikou (HK), Nanning (NN) and Shenzhen (SZ); ^c Mean indicates the monthly average value; ^d SIM indicates the simulation results from WRF/Chem; ^e
376 OBS indicates the observation data; ^f COR indicates the correlation coefficients, with statistically significant at 95% confident level.
377

378

379 Above all, the WRF/Chem simulation accounting for the temporal and spatial distribution of
380 AH (Grd_AH) has a relatively good capability in simulating urban climate and air quality over
381 South China. So, the differences between the modeling results from Non_AH and Grd_AH can be
382 used to quantify the impacts of anthropogenic heat on meteorology and air pollution.

383 3.3 Impacts of AH on meteorological conditions

384 Fig. 4a-d, Fig. 5a-d, Fig. 6a-b and Fig. 6g-h show the impacts of AH on surface meteorology,
385 which are defined as the monthly-averaged differences of these meteorological factors between
386 Grd_AH and Non_AH (Grd_AH minus Non_AH) at the surface layer over the modeling domain 2.
387 Fig. 4e-f and Fig. 6c-f show the relevant vertical changes of the meteorological factors along the
388 cross-section from (19.1°N, 108.9°E) to (24.8°N, 114.7°E) which is shown as the solid line AB in
389 Fig. 1b. The vertical cross section analysis through the line AB is to discuss the different effects of
390 AH on ambient environment between the big (Guangzhou) and the relatively small (Haikou) city.
391



393

394 **Fig. 3. The spatial distributions of monthly-averaged differences for surface O₃ and PM₁₀ between Fix_AH**
395 **and Grd_AH (Fix_AH minus Grd_AH). (a) and (c) show changes in January. (b) and (d) illustrate**
396 **variations in July.**

397

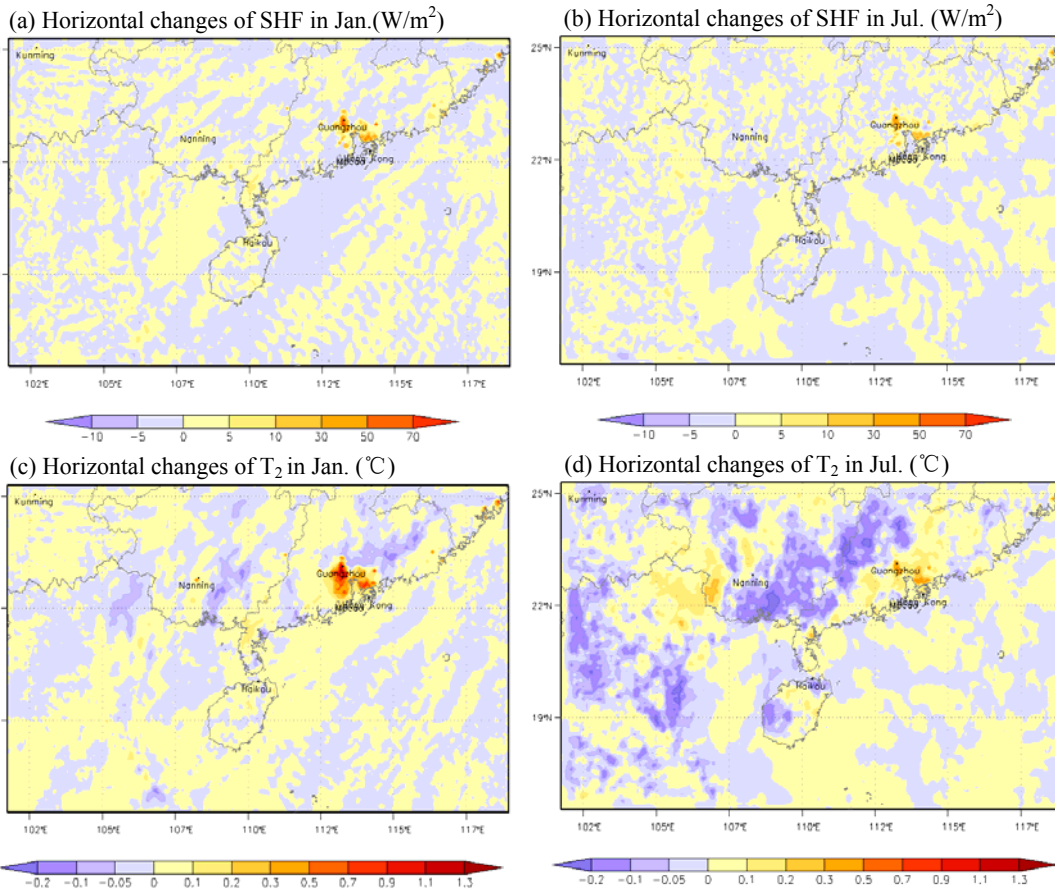
398 3.3.1 Changes of surface energy and air temperature

399 On account that AH and its diurnal variation are added to the sensible heat item in

400 WRF/Chem, the adding of gridded AH fluxes should increase the modeling results of sensible heat
 401 fluxes (SHF) over South China. As shown in Fig. 4a and b, the spatial patterns of SHF changes in
 402 both January and July are similar to the spatial distribution of AH fluxes presented in Fig. 2f. The
 403 significant increments ($> 10 \text{ W/m}^2$) of SHF over South China usually occur in and around
 404 mega-cities. Especially in the PRD city cluster, adding AH can cause SHF to increase by over 50
 405 W/m^2 in both January and July.

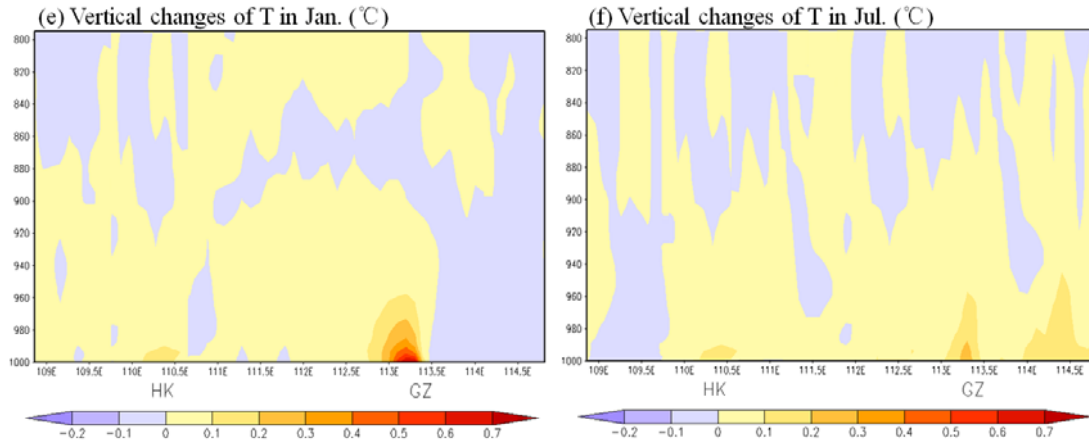
406 For the 2-m air temperature (T_2) over South China, the AH fluxes can increase their values
 407 by adding more surface heat into the atmosphere. As presented in Fig. 4c and d, the patterns of the
 408 monthly-averaged T_2 changes are similar to those of SHF (Fig. 4a and b). In the urban areas, the
 409 adding of AH can lead to the significant increase of T_2 , which may enhance the Urban Heat Islands
 410 (UHI). For example, the UHI intensity (the difference of monthly mean temperature between the
 411 maximum in urban areas and the minimum in surrounding rural areas) in PRD is about 1.7°C in
 412 January and 1.3°C in July for Non_AH case, while it increases to 2.4°C in January and 1.8°C in
 413 July for Grd_AH case. The maximum T_2 changes are usually found in the city centers of the PRD
 414 region, with the typical increments over 1.1 °C in January and over 0.5°C in July. These findings
 415 are comparable to the values estimated for other cities (Fan and Sailor, 2005; Ferguson and
 416 Woodbury, 2007; Chen et al., 2009; Zhu et al., 2010; Menberg et al., 2013; Wu and Yang, 2013;
 417 Bohnenstengel et al., 2014; Yu et al., 2014; Xie et al., 2016), and can be confirmed by the similar
 418 researches in South China (Meng et al., 2011; Feng et al., 2012; 2014).

419



420

421



422

423 **Fig. 4. The monthly-averaged differences between Grd_AH and Non_AH (Grd_AH minus Non_AH) for (a),**
 424 **(b) the spatial distribution of sensible heat flux (SHF); (c), (d) the spatial distribution of 2-m air temperature**
 425 **(T_2); (e), (f) the vertical distribution of air temperature (T) from the surface to the 800hPa layer along the**
 426 **line AB shown in Fig. 1b. Grd_AH and Non_AH represent the simulations with and without AH fluxes. (a),**
 427 **(c), and (e) show changes in January, while (b), (d), and (f) illustrate variations in July. In (e) and (f), HK**
 428 **and GZ are the abbreviations for Haikou and Guangzhou, respectively.**

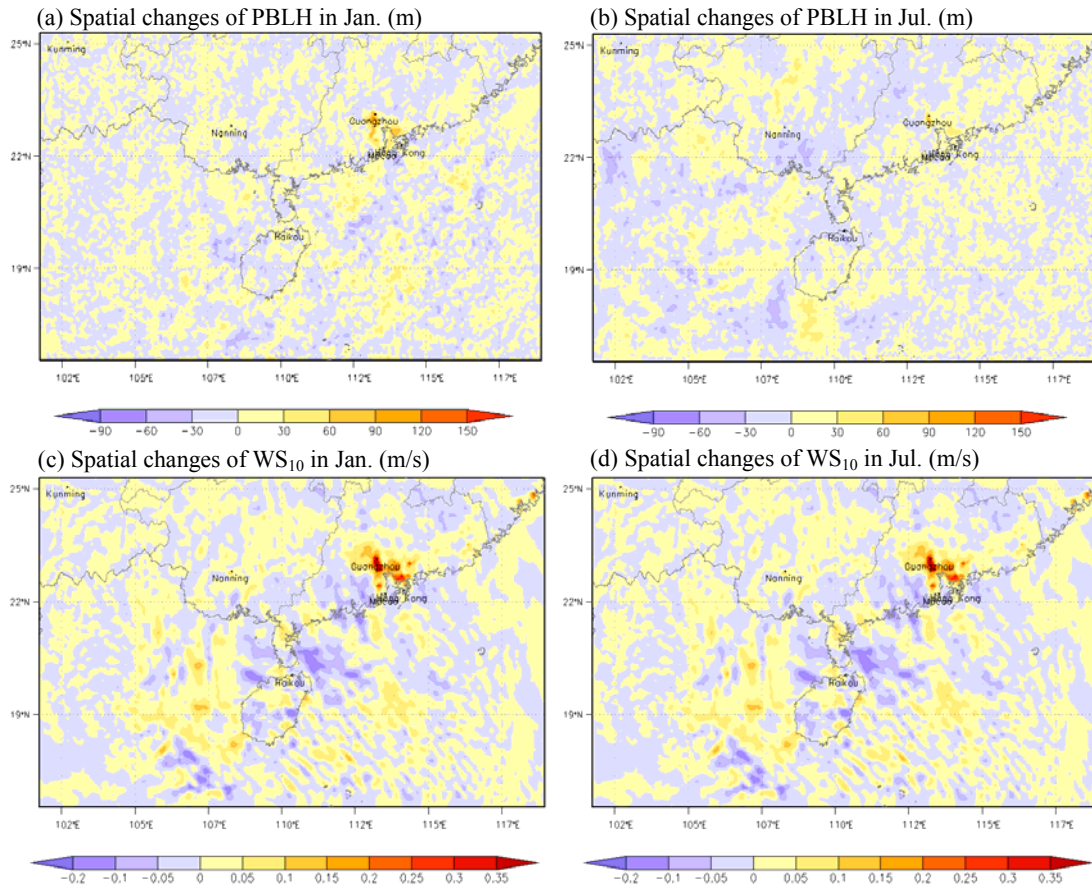
429

430 Fig. 4e and f present the vertical changes of air temperature from the surface to the 800hPa
 431 layer along the line AB (shown in Fig. 1b), and illustrate that the increases of air temperature
 432 causing by adding AH are mainly confined near the surface around the cities (Guangzhou and
 433 Haikou). These changes of air temperature in Guangzhou are more obvious than those in Haikou,
 434 because the AH emissions are much higher in Guangzhou. Furthermore, T_2 changes in winter (Fig.
 435 4e) are more obvious than those in summer (Fig. 4f), with the monthly mean increment of T over
 436 0.7°C for January while only around 0.4°C for July in Guangzhou. This phenomenon should be
 437 related with the fact that the background heat fluxes are much lower in winter so that the relative
 438 increase of T is more obvious.

439 3.3.2 Changes of boundary layer and wind field

440 The warming up of surface air temperature can enhance the vertical air movement in
 441 boundary layer (PBL), and thereby can increase the height of boundary layer (PBLH) as well. As
 442 shown in Fig. 5a and b, the boundary layer height becomes higher when the AH fluxes are taken
 443 into account. The big increments (more than 50m) usually occur in the urban areas of the PRD
 444 region. Because relative higher temperature increment in January can induce higher PBL in this
 445 cold season, the maximum changing values of PBLH can be 120m for January but only 90m for
 446 July.

447



448
449
450 **Fig. 5. The monthly-averaged differences of the height of planetary boundary layer (PBLH) and 10-m wind**
451 **speed (WS_{10}) between Grd_AH and Non_AH (Grd_AH minus Non_AH). Grd_AH and Non_AH represent**
452 **the simulations with and without AH fluxes. (a) and (c) show changes in January, while (b) and (d) illustrate**
453 **variations in July.**

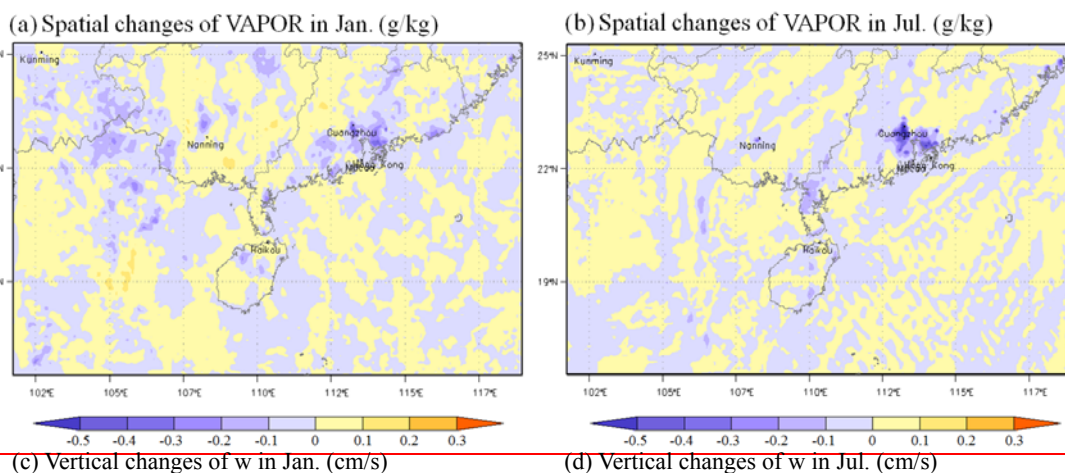
454
455 Fig. 5c and d show the changes in the 10-m wind speed over South China. Obviously, adding
456 AH can enhance the surface wind in the urban areas. The maximum increase is located in the PRD
457 region, with the values over 0.35 m/s in January and 0.3 m/s in July. In other cities like Chaozhou,
458 Nanning and Haikou, the increments are merely about 0.1 m/s. The warming of air temperature
459 near surface as well as the rising of PBLH induced by adding AH in cities can generate an
460 enhanced urban-breeze circulation. In previous studies, the increases in surface wind speed were
461 considered to be related with this strengthened urban-breeze circulation (Chen et al., 2009; Ryu et
462 al., 2013; Yu et al., 2014; Xie et al., 2016). Our results show that the vertical wind velocities
463 above the Guangzhou and Haikou is enhanced in both January and July (Fig. 6c and d), and the
464 simulated convergence at the surface near these cities increases by 0.04-0.13 /s in January and
465 0.05-0.18 /s in July (not shown). Consequently, we deduce that the enhanced vertical air
466 movement causes the surface stronger convergence and thereby induces higher surface wind speed.
467 It is worth mentioning that the changes of vertical air movement and surface wind may affect the
468 local land-sea breeze circulation in the coastal cities. For example, AH emission in Haikou
469 enhances the upward air movement above the city (Fig. 6c and d), causes the downward
470 movement above the surrounding waters (Fig. 6c and d), and increases the surface wind from sea

471 to land (stronger convergence). These changes imply that AH might strengthen sea breeze in the
472 daytime and weaken land breeze at night.

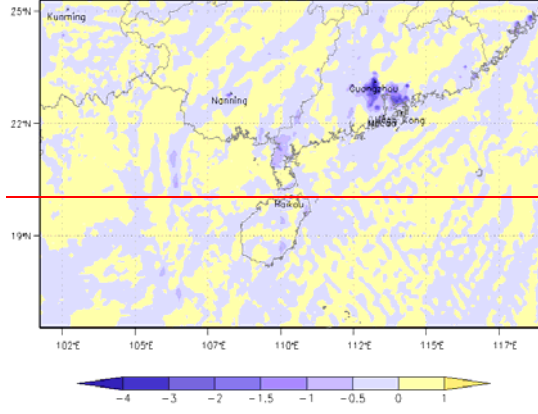
473 3.3.3 Changes of moisture and rainfall

474 Fig. 6a and b presents the monthly-averaged differences of water vapor mixing ratio
475 (VAPOR) at 2-m relative humidity (RH₂) between Grd_AH and Non_AH. Obviously, the air near
476 the surface of cities becomes dryer. The negative centers occur in the PRD region, the Chao-Shan
477 area, and some other cities, such as Haikou and Nanning. These cities which are also the AH
478 emission centers occurring in Fig. 2f. In the urban areas of PRD, in and around these cities, the
479 reductions of surface VAPOR of surface RH₂ are can be -30.1 to -4% -0.3 g/kg in January and
480 -10.2% to -2% 0.5 g/kg in July.

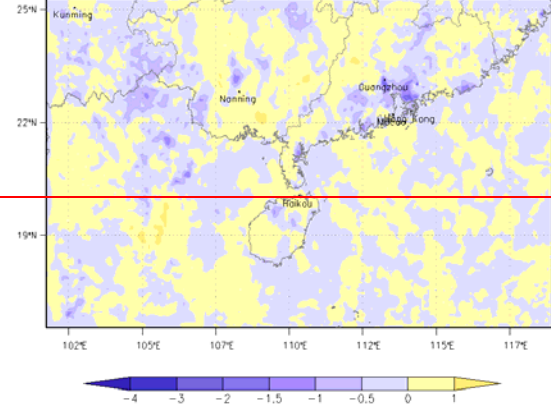
481 It was reported that the enhanced vertical air movement can transport more moisture from the
482 surface to the upper layer, and thereby can modify the spatial and vertical distributions of moisture
483 (Xie et al., 2016). This effect mechanism can be clearly illustrated by Fig. 6c-f in this study. As
484 shown in Fig. 6c and d, the vertical wind velocities above Guangzhou and Haikou increase by the
485 values of 0.2 – 0.5 cm/s in January and 0.5 - 1.0 cm/s in July, whereas w decreases in the rural
486 areas with the reductions about -0.3m/s in January and over -0.5 cm/s in July. This pattern means
487 that there are a strengthened upward air flow in cities and a strengthened downward air flow in the
488 surrounding areas, implying that the adding of AH fluxes makes the atmosphere more unstable and
489 tends to form deep convections in troposphere. So, as shown in Fig. 6e and f, more moisture can
490 be transported from the surface to the upper layers. In Guangzhou, for example, the water vapor
491 mixing ratios at the ground level decrease by -0.3g/kg in January and -0.5 g/kg in July, while those
492 at the upper PBL increase by 0.1 g/kg in January and 0.3 g/kg in July. The impact of AH on water
493 vapor is stronger in July. This seasonal difference can be ascribed to the facts that the atmosphere
494 is more stagnant and dryer in winter and more convective and wetter in summer. Furthermore, the
495 changes in Haikou are generally smaller than those in Guangzhou, which can be explained by the
496 fact that the AH emissions are much lower in Haikou.



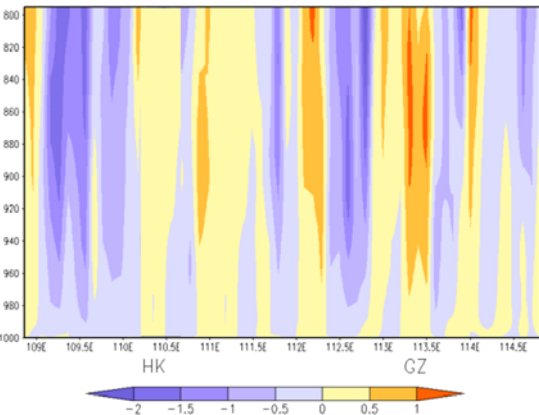
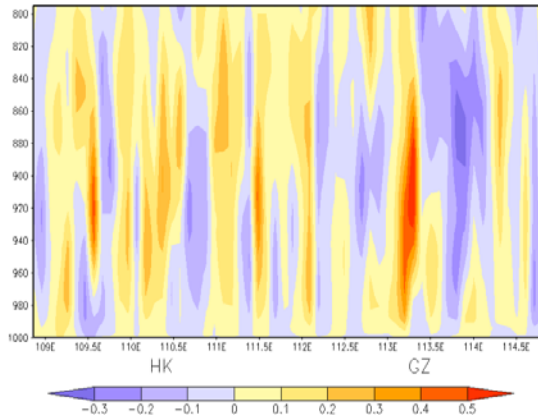
(a) Spatial changes of RH₂ in Jan. (%)



(b) Spatial changes of RH₂ in Jul. (%)

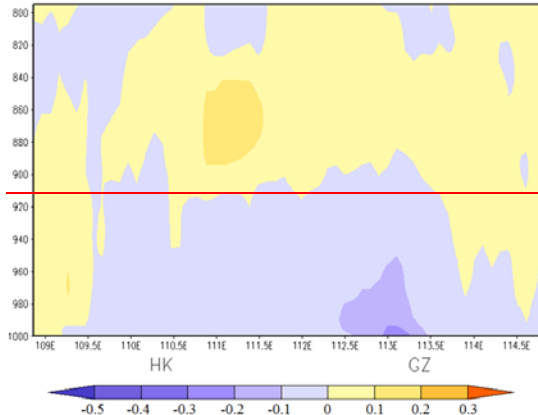


499

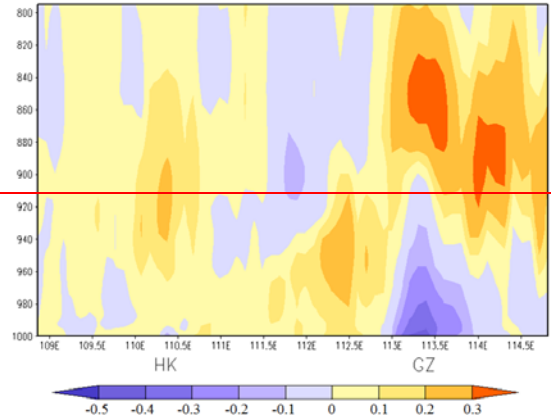


500

(e) Vertical changes of VAPOR in Jan. (g/kg)

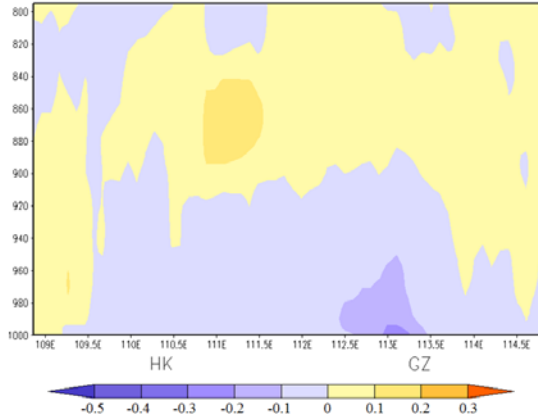


(f) Vertical changes of VAPOR in Jul. (g/kg)

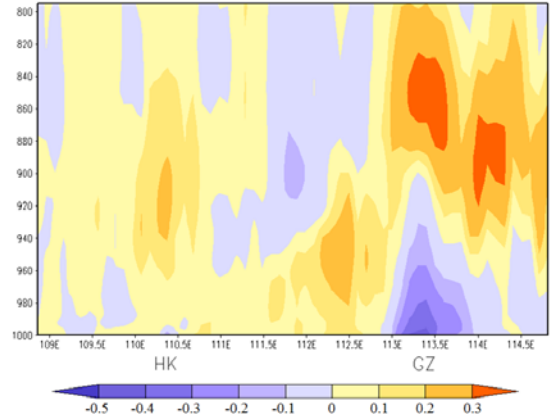


501

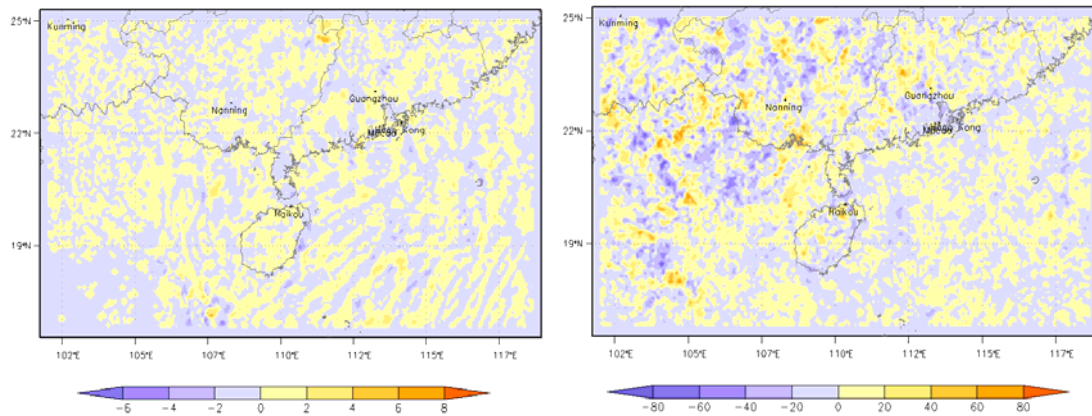
(g) Spatial changes of RAIN in Jan. (mm):g



(h) Spatial changes of RAIN in Jul. (mm):g



502



503

504

505

506

507

508

509

510

511

512

Fig. 6. The monthly-averaged differences between Grd_AH and Non_AH (Grd_AH minus Non_AH) for (a), (b) the spatial distribution of ~~water vapor mixing ratio (VAPOR) at 2-m relative humidity (RH₂)~~; (c), (d) the vertical distribution of vertical wind velocity (w); (e), (f) the vertical distribution of ~~water vapor mixing ratio (VAPOR)~~; (g), (h) the spatial distribution of precipitation (RAIN). The vertical cross section is from the surface to the 800hPa layer along the line AB shown in Fig. 1b. Grd_AH and Non_AH represent the simulations with and without AH fluxes. (a), (c), (e), and (g) show changes in January, while (b), (d), (f), and (g) illustrate variations in July. In (c), (d), (e), and (f), HK and GZ are the abbreviations for Haikou and Guangzhou, respectively.

513

514

515

516

517

518

519

520

521

More moisture transported from surface into the mid-troposphere can increase the precipitation in these urban areas as well. Fig. 6g and h illustrate the enhanced rainfall over South China both in January and July. Because of the negligible accumulative precipitation in winter, there are no significant differences between the Grd_AH and Non_AH simulations for rainfall in January. But in July, the increment of rainfall can be more than 50mm in and around big cities. Moreover, according to the dominant southeast wind in summer, the moisture can be transported to the downwind areas of the PRD city cluster, which causes the increases of rainfall in the northwest part of Guangdong province with the maximum value over 80 mm.

522

3.3.4 Diurnal pattern of the changes

523

524

525

526

527

528

529

530

531

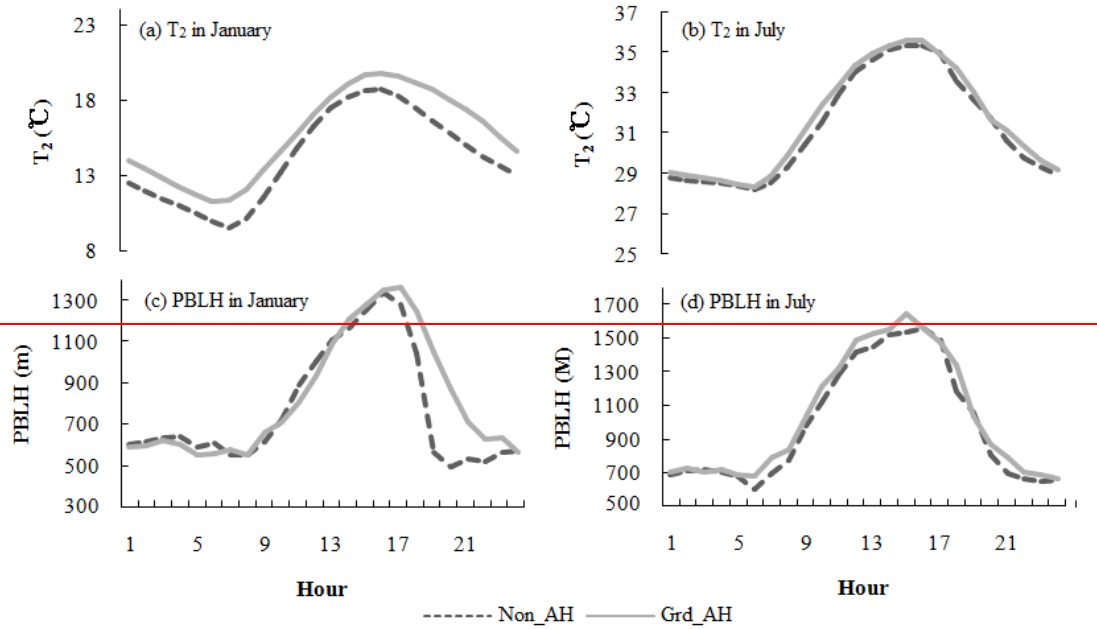
532

533

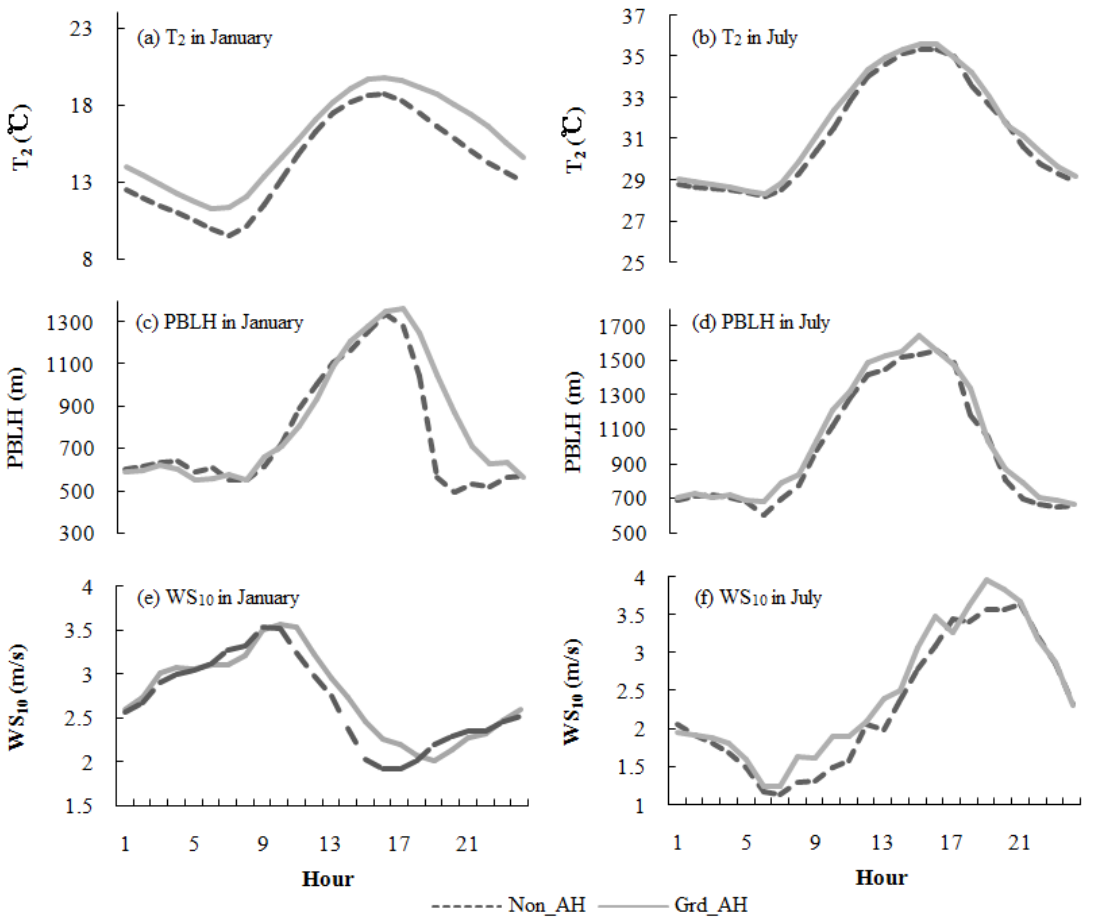
In order to better understand the different impacts of AH in the daytime and at night, the monthly-averaged diurnal variations of ~~T₂ and~~ PBLH, and WS₁₀ in January and July over the urban areas in Guangzhou are calculated based on the results from Grd_AH and Non_AH. As shown in Fig. 7a and b, adding AH fluxes can lead to an obvious increase of 2-m air temperature in both months, with the daily mean increase of 1.5°C for January and 0.6 °C for July. The increment of T₂ at night in January (1.69°C) is larger than that in the daytime (1.31°C), whereas the changes during the whole day in July are all around 0.6°C, which suggests that AH can weaken the diurnal T₂ variation in winter. With respect to PBLH, the AH fluxes can also result in a higher boundary layer. In July (Fig. 7d), the increment of PBLH nearly keeps a constant value of 54m (4.7%) from morning till night. However, in January (Fig. 7c), the nighttime increase of PBLH is much higher than that in the daytime. This phenomenon may be related with the facts that the absolute PBLH values are lower and the air temperatures increase more in the winter nights. For

534 WS₁₀. AH emission causes it to increase 0.07 m/s in January and 0.15m/s in July. Most increases
 535 occur in the daytime. The effect of AH on surface wind is negligible at night, which may be
 536 related to the fact that the land breeze at night (from land to sea) hinders the surface convergence
 537 (from sea to land) caused by AH.

538



539



540

541 Fig. 7. The monthly-averaged diurnal variations for 2-m air temperature (T_2) ~~and~~, the height of planetary
 542 boundary layer (PBLH), ~~and 10-m wind speed (WS_{10})~~ over the urban areas in Guangzhou. Grd_AH and
 543 Non_AH represent the simulations with and without AH fluxes, respectively. (a), (c) and (e) show diurnal
 544 curves in January, while (b), (d) and (f) illustrate those in July.

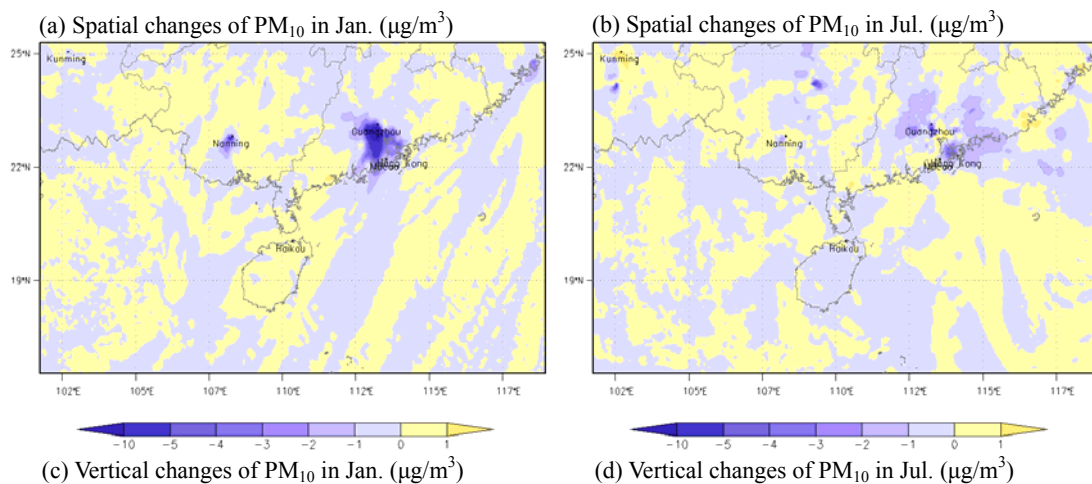
545

546 3.4 Impacts of AH on main air pollutants

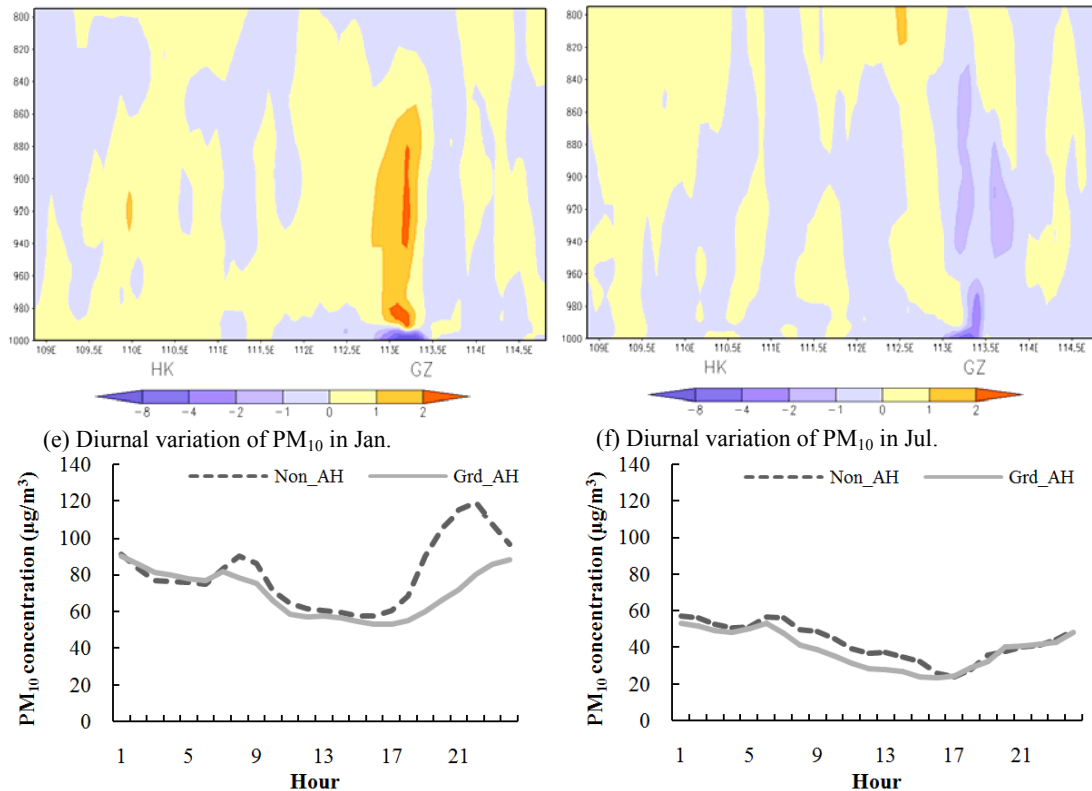
547 3.4.1 Changes of the spatial and vertical distribution of PM_{10}

548 Since adding AH changes the ~~meteorology~~ atmospheric conditions, it can affect the
 549 transportation and dispersion of air pollutants as well. Fig. 8a and b show the effects of AH on the
 550 spatial distribution of PM_{10} at the surface layer over South China in January and July. They
 551 illustrate that the concentrations of PM_{10} decrease in both season near the big cities, including the
 552 PRD city cluster, the Chao-shan area, and Nanning etc. The maximum reductions occur in the
 553 PRD region, with the monthly mean value over $-10\mu\text{g}/\text{m}^3$ for January and about $-5\mu\text{g}/\text{m}^3$ for July.
 554 Compared with the distribution of AH emissions as well as their effects on meteorological
 555 conditions, the main causes resulting in the reduction of surface PM_{10} should be attributed to the
 556 increase of PBLH, vertical upward air flow and surface wind speed, which can all facilitate PM_{10}
 557 transport and dispersion within the urban boundary layer. For another, as shown in Fig. 6h, the
 558 rainfall around the PRD cities can increase by 20-40% in July when the AH fluxes are taken into
 559 account, so the strengthened wet scavenging in summer may contribute to the decreases of the
 560 surface concentrations of PM_{10} as well. The surface reductions of PM_{10} induced by adding AH in
 561 the PRD region are smaller than those reported by Xie et al. (2016) in the Yangtze River Delta
 562 (YRD) region, which may attributed to the facts that the particle pollution is more severe and the
 563 AH emissions as well as their effects on meteorology are more obvious in the YRD region.

564



565



566

567

568

569

570

571

572

573

574

575

576

577

578

579

580

581

582

583

584

585

586

587

588

589

590

Fig. 8 Impacts of AH fluxes on the concentrations of PM₁₀: (a), (b) the spatial distribution of monthly-averaged differences for PM₁₀ between Grd_AH and Non_AH (Grd_AH minus Non_AH) at the surface layer; (c), (d) the vertical distribution of monthly-averaged differences for PM₁₀ between Grd_AH and Non_AH (Grd_AH minus Non_AH) from the surface to the 800hPa layer along the line AB shown in Fig. 1b; (e), (f) the monthly-averaged diurnal variations for PM₁₀ concentrations over the urban areas in Guangzhou. Grd_AH and Non_AH represent the simulations with and without AH fluxes. (a), (c), and (e) show changes in January, while (b), (d), and (f) illustrate variations in July. In (c) and (d), HK and GZ are the abbreviations for Haikou and Guangzhou, respectively.

Fig. 8c and d present the vertical plots for the changes of PM₁₀ impacted by adding AH (Grd_AH minus Non_AH) on the cross-sectional line AB shown in Fig. 1b. With respect to the megacity Guangzhou, the AH fluxes can decrease the concentrations of PM₁₀ near surface and increase those at the upper layers. This vertical change pattern of PM₁₀ is quite similar to that of water vapor (Fig. 6e and f), indicating that it is a reflection of the changes in vertical transport pattern due to AH (Yu et al., 2014; Xie et al., 2016). As shown in Fig. 8c for January, the decreases of PM₁₀ mainly confined at the surface, with the typical reductions over $-8\mu\text{g}/\text{m}^3$. Meanwhile, there are obvious increases of PM₁₀ concentrations at the upper levels, with the increments over $2\mu\text{g}/\text{m}^3$ from the 980hPa layer to the 850hPa layer (approximately from 500m to 1500m). But for July (Fig. 8d), from the surface to the 850hPa layer over Guangzhou, the PM₁₀ concentrations are all reduced over $-1\mu\text{g}/\text{m}^3$, with the maximum values over $-4\mu\text{g}/\text{m}^3$ on the ground. The increasing zones only occur at the upper layers above 1.5km, with the increments over $1\mu\text{g}/\text{m}^3$. This significant seasonal difference for the vertical distribution of PM₁₀ changes over Guangzhou should be related with the fact that the atmosphere is more unstable and convective in summer than in winter, which can be

591 further proven by the phenomenon that the enhanced upward air movement in July is stronger than
592 that in January (shown in Fig. 6e and f). It should be noted that the vertical changes of PM₁₀ in
593 Haikou are indistinctive, implying that the surface air pollutants cannot be remarkably affected by
594 adding AH if the heat emission fluxes are less than 10 w/m². Furthermore, the low particle
595 pollution level may be another cause for the negligible vertical changes of PM₁₀ in Haikou.

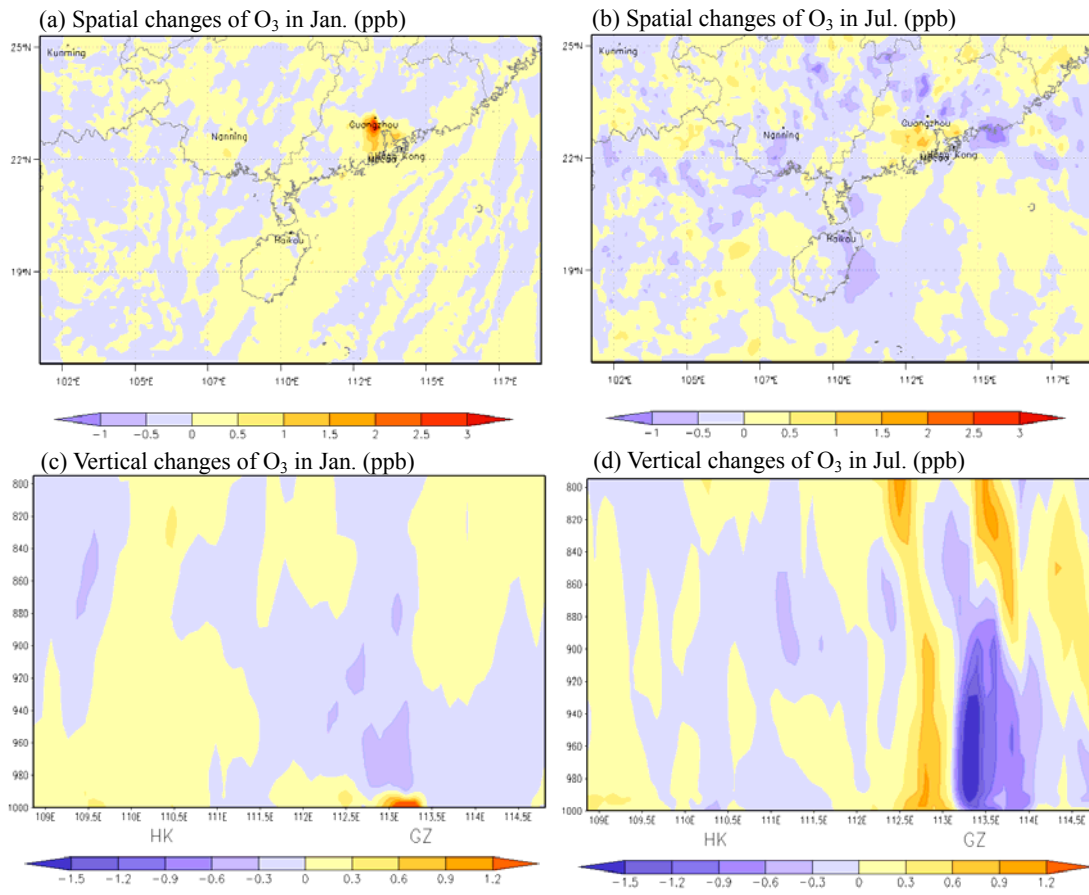
596 Fig. 8e and f show the monthly-averaged diurnal variations of surface PM₁₀ from the
597 Grd_AH and Non_AH simulations over the urban areas in Guangzhou. Obviously, the adding of
598 AH fluxes can lead to the decrease of surface PM₁₀ concentrations, with the daily mean value of
599 -10.4μg/m³ for January and -4.3μg/m³ for July. There are significant differences between the
600 impacts of AH in the daytime and those at night. In July (Fig. 8f), the decreases mainly occur from
601 6:00 to 17:00. In January (Fig. 8e), the decreases are -8.8μg/m³ from 8:00 to 18:00 and -11.9μg/m³
602 from 19:00 to 7:00, with the maximum reduction of -36.9μg/m³ at 21:00. This pattern has a
603 reverse correlation with the changes of PBLH shown in Fig. 7c and d, which also manifests the
604 important role of vertical air movement in the changes of PM₁₀.

605 **3.4.2 Changes of the spatial and vertical distribution of O₃**

606 Fig. 9a and b present the effects of AH on the spatial distribution of O₃ at the surface layer
607 over South China. The results show that the increases of surface O₃ level can be seen in megacities
608 for both January and July. In January (Fig. 9a), the maximum O₃ differences occur in the big cities
609 of the PRD region, with the monthly mean increment over 2.5ppb. In July (Fig. 9b), the increasing
610 areas become larger, but with the high values close to 1 ppb in and around the cities. This
611 changing pattern is similar to the findings reported in Seoul (Ryu et al., 2013), Beijing (Yu et al.,
612 2014) and the cities in the YRD region (Xie et al., 2016).

613 Fig. 9c and d show the effects of AH on the vertical distribution of O₃ from the surface to the
614 800hPa layer along the line AB (illustrated in Fig. 1b). For the urban areas of Haikou, the vertical
615 changes of O₃ are all within ±0.2 ppb, which means that low AH emissions in this city (<10w/m²)
616 cannot remarkably affected the physical and chemical formation of O₃. However, over the urban
617 areas of big city Guangzhou, the vertical distribution of O₃ concentrations can be noticeably
618 changed. In January (Fig. 9c), O₃ increases at the surface while decreases at the upper levels. The
619 increases of O₃ concentrations are limited within 300m above the surface (<995hPa) over the
620 urban areas, with the high values over 2.5 ppb. The maximum decreases of O₃ concentrations
621 occur from the 990hPa layer to the 860hPa layer (approximately from 400m to 1500m), and the
622 typical reductions are about 0.3 ppb. This change pattern in winter for Guangzhou is similar to the
623 findings reported in Shanghai and Hangzhou (Xie et al., 2016). But for July, the vertical change
624 pattern of O₃ above Guangzhou is totally different. As illustrated in Fig. 9d, O₃ concentrations
625 decrease at the lower layers while increase at the upper levels. The decreases occur from the
626 surface to the 850hPa layer (about 1.5 km) with the reduction values of -1 to -1.5ppb, and the
627 increases appear at the upper layers as well as the surrounding air columns around Guangzhou
628 with the increment about 0.9-1.2 ppb.

629



630

631

632 **Fig. 9. Impacts of AH fluxes on the concentrations of O₃: (a), (b) the spatial distribution of**
 633 **monthly-averaged differences for O₃ between Grd_AH and Non_AH (Grd_AH minus Non_AH) at the**
 634 **surface layer; (c), (d) the vertical distribution of monthly-averaged differences for O₃ between**
 635 **Grd_AH and Non_AH (Grd_AH minus Non_AH) from the surface to the 800hPa layer along the line AB shown in Fig. 1b.**
 636 **Grd_AH and Non_AH represent the simulations with and without AH fluxes. (a) and (c) show changes in**
 637 **January, while (b) and (d) illustrate variations in July. In (c) and (d), HK and GZ are the abbreviations for**
 638 **Haikou and Guangzhou, respectively.**

639

640 The mechanism how the AH fluxes influence the spatial and vertical distribution of O₃ is
 641 more complicated than that for PM₁₀. Only taking the physical effects that just impact O₃ transport
 642 and dispersion into account, we can merely deduce that O₃ is seemingly reduced at the surface and
 643 may increase at the upper layers, because the increase of surface wind speed can facilitate O₃
 644 advection transport and the rising up of PBLH can lead to O₃ dilution. However, O₃ is a secondary
 645 air pollutant produced by a series of complex chemical reactions that are also deeply affected by
 646 the ambient meteorological conditions. So, the chemical effects can play an important role in O₃
 647 changes as well. For example, the increases of air temperature induced by adding AH can
 648 accelerate O₃ production rate. So it can directly increase the O₃ concentrations near the surface
 649 (referred to as the direct chemical effect hereafter). Moreover, because of the O₃ sensitivity in the
 650 daytime and the NO_x titration at night, O₃ formation is inextricably linked with NO_x (referred to as
 651 indirect chemical effect hereafter). As shown in Fig. 10, due mainly to the increases of PBLH and

652 upward air flow caused by adding AH, NO_x can decrease at ground level and increase at upper
653 layers in both January and July. Then when the process of NO_x titration predominate the O_3
654 chemistry at night, less NO_x consumes less O_3 and leaves more O_3 at the surface while more NO_x
655 consumes more O_3 and reduce O_3 at the upper layers. For the daytime, because O_3 formation is
656 sensitive to VOC over the cities in South China (Xie et al., 2014), the decrease in surface NO_x can
657 lead to a slight increase in O_3 while the increase of NO_x at upper layers can result in the O_3
658 decrease. In January over Guangzhou, these direct and indirect chemical effects should play a
659 more important role in O_3 changes than the physical effects, and thereby O_3 increases at ground
660 level and decreases at upper layers. But in July, the physical effects should be the governing factor
661 and cause the different pattern of O_3 changes in Guangzhou.

662 In the previous study on the O_3 variations induced by adding AH, it was found that the
663 vertical changing patterns of O_3 over the YRD region in both January and July are always the
664 same as the pattern shown in the winter of Guangzhou (Xie et al., 2016). Comparing the vertical
665 changes of w for July in Guangzhou and those in Shanghai or Hangzhou, we can tell that the AH
666 fluxes can induce stronger upward air movement in the cities of South China, which may be
667 related with their special topographic and climatic features, and thereby more O_3 below the
668 850hPa layer is transported to the upper layers or to the surrounding areas of Guangzhou. On the
669 other hand, the rise of air temperature is smaller in Guangzhou than those in the YRD cities, so
670 there is no enough produced O_3 to compensate the loss of O_3 on the ground. Consequently,
671 impacted by adding AH, O_3 decreases at the surface while increases at the upper layers in the
672 summer of Guangzhou.

673

674 **4. Conclusions**

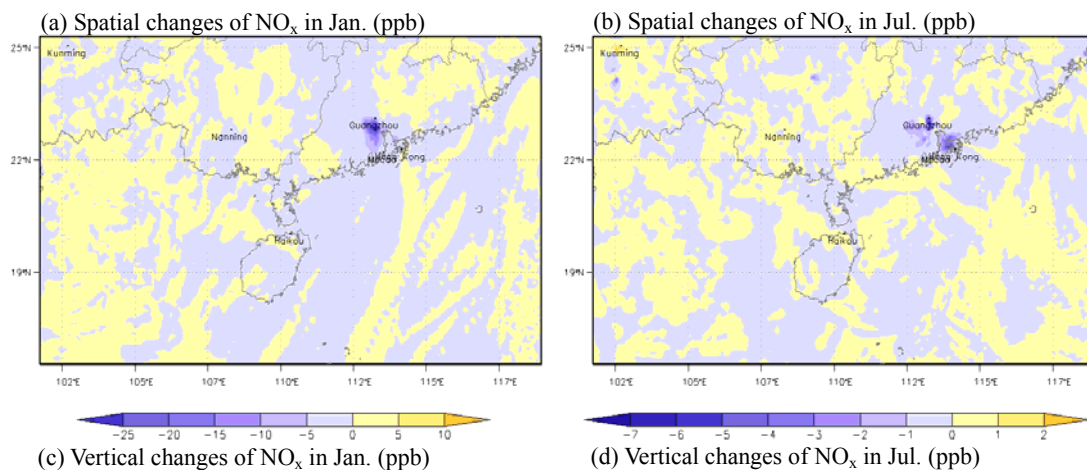
675 Anthropogenic heat (AH) fluxes related with the human activities can change the urban
676 circulation and thereby affect the air pollution in and around cities. In this paper, we carry out
677 systematic analyses to study the changes of meteorological conditions induced by AH and their
678 effects on the concentrations of PM_{10} , NO_x and O_3 in South China. Firstly, the temporal and spatial
679 distribution of AH emissions is estimated by a top-down energy inventory method. Secondly, the
680 AH parameterization in WRF/Chem is modified to adopt the gridded AH data with the temporal
681 variation. Finally, the WRF/Chem simulations are performed, and the differences between the
682 cases with and without adding AH are analyzed to quantify the impacts of AH.

683 The results show that high AH fluxes generally occur in and around the cities. In 2014, the
684 regional mean values of AH over Guangdong, Guangxi and Hainan province are 1.68, 0.44 and
685 0.49 W/m^2 , while the typical values in the urban areas of the PRD region can reach 58.03 W/m^2 .
686 The model results of WRF/Chem fit the observations well. Adding the gridded AH emissions can
687 better describe the heterogeneous impacts of AH on regional meteorology and air quality. When
688 AH fluxes are taken into account, the urban heat island and urban-breeze circulations in the big
689 cities are significantly changed. In the PRD city cluster, 2-m air temperature rises up by 1.1°C in

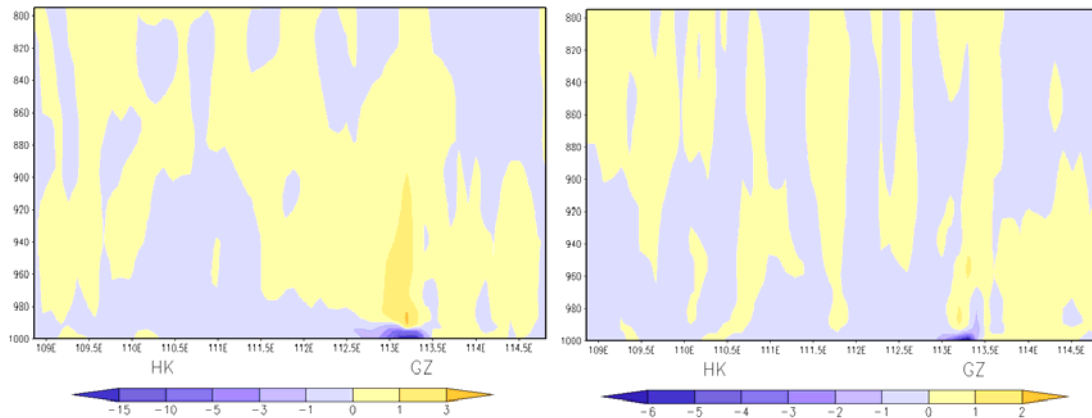
690 January and over 0.5°C in July, the boundary layer height increases by 120m in January and 90m
 691 in July, and 10-m wind speed is enhanced over 0.35 m/s in January and 0.3 m/s in July. The
 692 enhanced vertical movement can transport more moisture to higher levels, and causes the
 693 accumulative precipitation to increase by 20-40% over the megacities in July. Influenced by the
 694 modifications of meteorological conditions, the spatial and vertical distribution of air pollutants is
 695 modified as well. The concentrations of PM_{10} and NO_x decrease near surface while increase at the
 696 upper levels over the big cities in the PRD region, which are mainly related with the higher PBLH,
 697 stronger upward air flow, and higher surface wind speed. Because the direct chemical effect (the
 698 rising up of air temperature directly accelerates surface O_3 formation) and the indirect chemical
 699 effect (the decrease in NO_x at the ground results in the increase of surface O_3) play a more
 700 important role than the physical effects in winter, the surface O_3 concentrations can increase in
 701 January with maximum changes over 2.5ppb in the megacities. However, in July, the vertical
 702 changes of O_3 concentrations induced by adding AH show a different pattern, with reductions at
 703 the lower layers and increments at the upper layers over Guangzhou. This phenomenon should be
 704 attributed to the fact that the physical effects (enhanced upward movement caused by AH) become
 705 the dominant factor in summer.

706 There is an important question asked many times by scientists about whether anthropogenic
 707 heat emissions contribute to global warming. Although the answers are probably negative, the
 708 systematic analyses of AH over South China in this paper can enhance the understanding of the
 709 magnitude of AH emission from megacities and its impact on regional meteorology and
 710 atmospheric chemistry. Compared with the effects from urban land use (Wang et al., 2007; 2009b;
 711 Feng et al., 2012; Chen et al., 2014b; Li et al., 2014; 2016; Liao et al., 2015; Zhu et al., 2015), the
 712 impacts of AH are relative small. Especially in some cities with less air pollution and AH
 713 emissions, such as Haikou, the effects of AH on air quality may be ignored. But our results also
 714 clearly show that the meteorology and air pollution predictions in and around big cities are highly
 715 sensitive to the anthropogenic heat inputs. Thus, for further understanding of urban atmospheric
 716 environment issues, more studies of the anthropogenic heat release in megacities should be better
 717 considered.

718



719



720
 721 **Fig. 10. Impacts of AH fluxes on the concentrations of NO_x: (a), (b) the spatial distribution of**
 722 **monthly-averaged differences for NO_x between Grd_AH and Non_AH (Grd_AH minus Non_AH) at the**
 723 **surface layer; (c), (d) the vertical distribution of monthly-averaged differences for NO_x between Grd_AH**
 724 **and Non_AH (Grd_AH minus Non_AH) from surface to 800 hPa layer along the line AB shown in Fig. 1b.**
 725 **Grd_AH and Non_AH represent the simulations with and without AH fluxes. (a) and (c) show changes in**
 726 **January, while (b) and (d) illustrate variations in July. In (c) and (d), HK and GZ are the abbreviations for**
 727 **Haikou and Guangzhou, respectively.**

728
 729 **Acknowledgments**

730 This work was supported by the National Natural Science Foundation of China (41475122,
 731 91544230, [41621005](#)), Key Laboratory of South China Sea Meteorological Disaster Prevention
 732 and Mitigation of Hainan Province (SCSF201401), the National Special Fund for Environmental
 733 Protection Research in the Public Interest (201409008), ~~the National Science Foundation of~~
 734 ~~Jiangsu Province (BE2015151)~~, and EU 7th Framework Marie Curie Actions IRSES project
 735 REQUA (PIRSSES-GA-2013-612671). The authors would like to thank the anonymous reviewers
 736 for their constructive and precious comments on this manuscript.

737
 738 **References**

739 Ackermann, I. J., Hass, H., Memmesheimer, M., Ebel, A., Binkowski, F. S., and Shankar, U.: Modal aerosol
 740 dynamics model for Europe: Development and first applications, *Atmos Environ*, 32, 2981-2999, Doi
 741 10.1016/S1352-2310(98)00006-5, 1998.
 742 Akbari, H., Pomerantz, M., and Taha, H.: Cool surfaces and shade trees to reduce energy use and improve air
 743 quality in urban areas, *Sol Energy*, 70, 295-310, Doi 10.1016/S0038-092x(00)00089-X, 2001.
 744 Allen, L., Lindberg, F., and Grimmond, C. S. B.: Global to city scale urban anthropogenic heat flux: model and
 745 variability, *International Journal Of Climatology*, 31, 1990-2005, 10.1002/joc.2210, 2011.
 746 Balzarini, A., Pirovano, G., Honzak, L., Zabkar, R., Curci, G., Forkel, R., Hirtl, M., San Jose, R., Tuccella, P., and
 747 Grell, G. A.: WRF-Chem model sensitivity to chemical mechanisms choice in reconstructing aerosol optical
 748 properties, *Atmos Environ*, 115, 604-619, 10.1016/j.atmosenv.2014.12.033, 2015.
 749 Block, A., Keuler, K., and Schaller, E.: Impacts of anthropogenic heat on regional climate patterns, *Geophys Res*
 750 *Lett*, 31, Artn L12211_ [10.1029/2004gl019852](#), 2004.
 751
 752 Bohnenstengel, S. I., Hamilton, I., Davies, M., and Belcher, S. E.: Impact of anthropogenic heat emissions on
 753 London's temperatures, *Q J Roy Meteor Soc*, 140, 687-698, 10.1002/qj.2144, 2014.

754 Chan, C. K., and Yao, X.: Air pollution in mega cities in China, *Atmos Environ*, 42, 1-42,
755 10.1016/j.atmosenv.2007.09.003, 2008.

756 Chen, F., and Dudhia, J.: Coupling an advanced land surface-hydrology model with the Penn State-NCAR MM5
757 modeling system. Part I: Model implementation and sensitivity, *Mon Weather Rev*, 129, 569-585, Doi
758 10.1175/1520-0493(2001)129<0569:Caalsh>2.0.Co;2, 2001.

759 Chen, Y., Jiang, W. M., Zhang, N., He, X. F., and Zhou, R. W.: Numerical simulation of the anthropogenic heat
760 effect on urban boundary layer structure, *Theor Appl Climatol*, 97, 123-134, 10.1007/s00704-008-0054-0, 2009.

761 Chen, F., Kusaka, H., Bornstein, R., Ching, J., Grimmond, C. S. B., Grossman-Clarke, S., Loridan, T., Manning, K.
762 W., Martilli, A., Miao, S. G., Sailor, D., Salamanca, F. P., Taha, H., Tewari, M., Wang, X. M., Wyszogrodzki, A.
763 A., and Zhang, C. L.: The integrated WRF/urban modelling system: development, evaluation, and applications to
764 urban environmental problems, *International Journal Of Climatology*, 31, 273-288, 10.1002/joc.2158, 2011.

765 Chen, B., Shi, G. Y., Wang, B., Zhao, J. Q., and Tan, S. C.: Estimation of the anthropogenic heat release
766 distribution in China from 1992 to 2009, *Acta Meteorol Sin*, 26, 507-515, 10.1007/s13351-012-0409-y, 2012.

767 Chen, B., Dong, L., Shi, G. Y., Li, L. J., and Chen, L. F.: Anthropogenic Heat Release: Estimation of Global
768 Distribution and Possible Climate Effect, *J Meteorol Soc Jpn*, 92A, 157-165, 10.2151/jmsj.2014-A10, 2014a.

769 Chen, B., Yang, S., Xu, X. D., and Zhang, W.: The impacts of urbanization on air quality over the Pearl River
770 Delta in winter: roles of urban land use and emission distribution, *Theor Appl Climatol*, 117, 29-39,
771 10.1007/s00704-013-0982-1, 2014b.

772 Civerolo, K., Hogrefe, C., Lynn, B., Rosenthal, J., Ku, J. Y., Solecki, W., Cox, J., Small, C., Rosenzweig, C.,
773 Goldberg, R., Knowlton, K., and Kinney, P.: Estimating the effects of increased urbanization on surface
774 meteorology and ozone concentrations in the New York City metropolitan region, *Atmos Environ*, 41,
775 1803-1818, 10.1016/j.atmosenv.2006.10.076, 2007.

776 Crutzen, P. J.: New Directions: The growing urban heat and pollution "island" effect - impact on chemistry and
777 climate, *Atmos Environ*, 38, 3539-3540, 10.1016/j.atmosenv.2004.03.032, 2004.

778 Fan, H. L., and Sailor, D. J.: Modeling the impacts of anthropogenic heating on the urban climate of Philadelphia:
779 a comparison of implementations in two PBL schemes, *Atmos Environ*, 39, 73-84,
780 10.1016/j.atmosenv.2004.09.031, 2005.

781 Fang, M., Chan, C. K., and Yao, X. H.: Managing air quality in a rapidly developing nation: China, *Atmos Environ*,
782 43, 79-86, 10.1016/j.atmosenv.2008.09.064, 2009.

783 Feng, J. M., Wang, Y. L., Ma, Z. G., and Liu, Y. H.: Simulating the Regional Impacts of Urbanization and
784 Anthropogenic Heat Release on Climate across China, *J Climate*, 25, 7187-7203, 10.1175/Jcli-D-11-00333.1,
785 2012.

786 Feng, J. M., Wang, J., and Yan, Z. W.: Impact of Anthropogenic Heat Release on Regional Climate in Three Vast
787 Urban Agglomerations in China, *Adv Atmos Sci*, 31, 363-373, 10.1007/s00376-013-3041-z, 2014.

788 Ferguson, G., and Woodbury, A. D.: Urban heat island in the subsurface, *Geophys Res Lett*, 34, Artn L23713,
789 10.1029/2007gl032324, 2007.

790 Flanner, M. G.: Integrating anthropogenic heat flux with global climate models, *Geophys Res Lett*, 36, Artn
791 L02801,
792 10.1029/2008gl036465, 2009.

793 Grell, G. A., and Devenyi, D.: A generalized approach to parameterizing convection combining ensemble and data
794 assimilation techniques, *Geophys Res Lett*, 29, Artn 1693,
795 10.1029/2002gl015311, 2002.

796 Grell, G. A., Peckham, S. E., Schmitz, R., McKeen, S. A., Frost, G., Skamarock, W. C., and Eder, B.: Fully
797 coupled "online" chemistry within the WRF model, *Atmos Environ*, 39, 6957-6975,
798 10.1016/j.atmosenv.2005.04.027, 2005.

799 | ~~Group, W. B.: East Asia's changing urban landscape: measuring a decade of spatial growth, World Bank,~~
800 | ~~Washington Dc, 2015.~~

801 | Guenther, A., Karl, T., Harley, P., Wiedinmyer, C., Palmer, P. I., and Geron, C.: Estimates of global terrestrial
802 | isoprene emissions using MEGAN (Model of Emissions of Gases and Aerosols from Nature), *Atmos Chem Phys*,
803 | 6, 3181-3210, 2006.

804 | Hamilton, I. G., Davies, M., Steadman, P., Stone, A., Ridley, I., and Evans, S.: The significance of the
805 | anthropogenic heat emissions of London's buildings: A comparison against captured shortwave solar radiation,
806 | *Build Environ*, 44, 807-817, 10.1016/j.buildenv.2008.05.024, 2009.

807 | Iamarino, M., Beevers, S., and Grimmond, C. S. B.: High-resolution (space, time) anthropogenic heat emissions:
808 | London 1970-2025, *International Journal Of Climatology*, 32, 1754-1767, 10.1002/joc.2390, 2012.

809 | Ichinose, T., Shimodozono, K., and Hanaki, K.: Impact of anthropogenic heat on urban climate in Tokyo, *Atmos*
810 | *Environ*, 33, 3897-3909, Doi 10.1016/S1352-2310(99)00132-6, 1999.

811 | Janjic, Z. I.: The Step-Mountain Eta Coordinate Model - Further Developments Of the Convection, Viscous
812 | Sublayer, And Turbulence Closure Schemes, *Mon Weather Rev*, 122, 927-945, Doi
813 | 10.1175/1520-0493(1994)122<0927:Tsmecm>2.0.Co;2, 1994.

814 | Jiang, X. Y., Wiedinmyer, C., Chen, F., Yang, Z. L., and Lo, J. C. F.: Predicted impacts of climate and land use
815 | change on surface ozone in the Houston, Texas, area, *J Geophys Res-Atmos*, 113, Artn D20312,
816 | 10.1029/2008jd009820, 2008.

817 | Kim, H. J., and Wang, B.: Sensitivity of the WRF Model Simulation of the East Asian Summer Monsoon in 1993
818 | to Shortwave Radiation Schemes and Ozone Absorption, *Asia-Pac J Atmos Sci*, 47, 167-180,
819 | 10.1007/s13143-011-0006-y, 2011.

820 | Lee, S. H., Song, C. K., Baik, J. J., and Park, S. U.: Estimation of anthropogenic heat emission in the Gyeong-In
821 | region of Korea, *Theor Appl Climatol*, 96, 291-303, 10.1007/s00704-008-0040-6, 2009.

822 | Li, M. M., Song, Y., Huang, X., Li, J. F., Mao, Y., Zhu, T., Cai, X. H., and Liu, B.: Improving mesoscale modeling
823 | using satellite-derived land surface parameters in the Pearl River Delta region, China, *J Geophys Res-Atmos*,
824 | 119, 6325-6346, 10.1002/2014JD021871, 2014.

825 | Li, M. M., Song, Y., Mao, Z. C., Liu, M. X., and Huang, X.: Impacts of thermal circulations induced by
826 | urbanization on ozone formation in the Pearl River Delta region, China, *Atmos Environ*, 127, 382-392,
827 | 10.1016/j.atmosenv.2015.10.075, 2016.

828 | Liao, J. B., Wang, T. J., Jiang, Z. Q., Zhuang, B. L., Xie, M., Yin, C. Q., Wang, X. M., Zhu, J. L., Fu, Y., and
829 | Zhang, Y.: WRF/Chem modeling of the impacts of urban expansion on regional climate and air pollutants in
830 | Yangtze River Delta, China, *Atmos Environ*, 106, 204-214, 10.1016/j.atmosenv.2015.01.059, 2015.

831 | Lin, Y. L., Farley, R. D., and Orville, H. D.: Bulk Parameterization Of the Snow Field In a Cloud Model, *J Clim*
832 | *Appl Meteorol*, 22, 1065-1092, Doi 10.1175/1520-0450(1983)022<1065:Bpotsf>2.0.Co;2, 1983.

833 | Liu, M., Wang, H., Wang, H., Oda, T., Zhao, Y., Yang, X., Zang, R., Zang, B., Bi, J., and Chen, J.: Refined
834 | estimate of China's CO2 emissions in spatiotemporal distributions, *Atmos Chem Phys*, 13, 10873-10882,
835 | 10.5194/acp-13-10873-2013, 2013a.

836 | Liu, Q., Lam, K. S., Jiang, F., Wang, T. J., Xie, M., Zhuang, B. L., and Jiang, X. Y.: A numerical study of the
837 | impact of climate and emission changes on surface ozone over South China in autumn time in 2000-2050, *Atmos*
838 | *Environ*, 76, 227-237, 10.1016/j.atmosenv.2013.01.030, 2013b.

839 | Lo, J. C. F., Lau, A. K. H., Chen, F., Fung, J. C. H., and Leung, K. K. M.: Urban modification in a mesoscale
840 | model and the effects on the local circulation in the Pearl River Delta region, *J Appl Meteorol Clim*, 46, 457-476,
841 | 10.1175/Jam2477.1, 2007.

842 | Lu, X., Chow, K. C., Yao, T., Lau, A. K. H., and Fung, J. C. H.: Effects of urbanization on the land sea breeze
843 | circulation over the Pearl River Delta region in winter, *International Journal Of Climatology*, 30, 1089-1104,

844 10.1002/joc.1947, 2010.

845 Lu, Y., Wang, Q. G., Zhang, Y. Y., Sun, P., and Qian, Y.: An estimate of anthropogenic heat emissions in China,
846 International Journal Of Climatology, 36, 1134-1142, 10.1002/joc.4407, 2016.

847 Madronich, S.: Photodissociation In the Atmosphere .1. Actinic Flux And the Effects Of Ground Reflections And
848 Clouds, J Geophys Res-Atmos, 92, 9740-9752, Doi 10.1029/Jd092id08p09740, 1987.

849 Menberg, K., Bayer, P., Zosseder, K., Rumohr, S., and Blum, P.: Subsurface urban heat islands in German cities,
850 Sci Total Environ, 442, 123-133, 10.1016/j.scitotenv.2012.10.043, 2013.

851 Meng, W. G., Zhang, Y. X., Li, J. N., Lin, W. S., Dai, G. F., and Li, H. R.: Application Of Wrf/Ucm In the
852 Simulation Of a Heat Wave Event And Urban Heat Island around Guangzhou, J Trop Meteorol, 17, 257-267,
853 10.3969/j.issn.1006-8775.2011.03.007, 2011.

854 Mirzaei, P. A., and Haghghat, F.: Approaches to study Urban Heat Island - Abilities and limitations, Build
855 Environ, 45, 2192-2201, 10.1016/j.buildenv.2010.04.001, 2010.

856 Mlawer, E. J., Taubman, S. J., Brown, P. D., Iacono, M. J., and Clough, S. A.: Radiative transfer for
857 inhomogeneous atmospheres: RRTM, a validated correlated-k model for the longwave, J Geophys Res-Atmos,
858 102, 16663-16682, Doi 10.1029/97jd00237, 1997.

859 Oke, T. R.: The Urban Energy-Balance, Prog Phys Geog, 12, 471-508, Doi 10.1177/030913338801200401, 1988.

860 Pigeon, G., Legain, D., Durand, P., and Masson, V.: Anthropogenic heat release in an old European agglomeration
861 (Toulouse, France), International Journal Of Climatology, 27, 1969-1981, 10.1002/joc.1530, 2007.

862 Quah, A. K. L., and Roth, M.: Diurnal and weekly variation of anthropogenic heat emissions in a tropical city,
863 Singapore, Atmos Environ, 46, 92-103, 10.1016/j.atmosenv.2011.10.015, 2012.

864 Rizwan, A. M., Dennis, Y. C. L., and Liu, C. H.: A review on the generation, determination and mitigation of
865 Urban Heat Island, J Environ Sci-China, 20, 120-128, Doi 10.1016/S1001-0742(08)60019-4, 2008.

866 Ryu, Y. H., Baik, J. J., and Lee, S. H.: Effects of anthropogenic heat on ozone air quality in a megacity, Atmos
867 Environ, 80, 20-30, 10.1016/j.atmosenv.2013.07.053, 2013.

868 Sailor, D. J., and Lu, L.: A top-down methodology for developing diurnal and seasonal anthropogenic heating
869 profiles for urban areas, Atmos Environ, 38, 2737-2748, 10.1016/j.atmosenv.2004.01.034, 2004.

870 Schell, B., Ackermann, I. J., Hass, H., Binkowski, F. S., and Ebel, A.: Modeling the formation of secondary
871 organic aerosol within a comprehensive air quality model system, J Geophys Res-Atmos, 106, 28275-28293, Doi
872 10.1029/2001jd000384, 2001.

873 Stockwell, W. R., Middleton, P., Chang, J. S., and Tang, X. Y.: The 2nd Generation Regional Acid Deposition
874 Model Chemical Mechanism for Regional Air-Quality Modeling, J Geophys Res-Atmos, 95, 16343-16367, Doi
875 10.1029/Jd095id10p16343, 1990.

876 Stone, B.: Urban sprawl and air quality in large US cities, J Environ Manage, 86, 688-698,
877 10.1016/j.jenvman.2006.12.034, 2008.

878 Wang, X. M., Lin, W. S., Yang, L. M., Deng, R. R., and Lin, H.: A numerical study of influences of urban
879 land-use change on ozone distribution over the Pearl River Delta region, China, Tellus B, 59, 633-641,
880 10.1111/j.1600-0889.2007.00271.x, 2007.

881 Wang, T., Wei, X. L., Ding, A. J., Poon, C. N., Lam, K. S., Li, Y. S., Chan, L. Y., and Anson, M.: Increasing
882 surface ozone concentrations in the background atmosphere of Southern China, 1994-2007, Atmos Chem Phys, 9,
883 6217-6227, 2009a.

884 Wang, X. M., Chen, F., Wu, Z. Y., Zhang, M. G., Tewari, M., Guenther, A., and Wiedinmyer, C.: Impacts of
885 Weather Conditions Modified by Urban Expansion on Surface Ozone: Comparison between the Pearl River
886 Delta and Yangtze River Delta Regions, Adv Atmos Sci, 26, 962-972, 10.1007/s00376-009-8001-2, 2009b.

887 [Wang, X. M., Liao, J. B., Zhang, J., Shen, C., Chen, W. H., Xia, B. C., and Wang, T. J.: A Numeric Study of
888 Regional Climate Change Induced by Urban Expansion in the Pearl River Delta, China, J Appl Meteorol Clim.](#)

889 | [53, 346-362, 2014.](#)

890 | [World Bank Group: East Asia's changing urban landscape: measuring a decade of spatial growth. World Bank,](#)

891 | [Washington Dc, 2015.](#)

892 | Wu, J. B., Chow, K. C., Fung, J. C. H., Lau, A. K. H., and Yao, T.: Urban heat island effects of the Pearl River

893 | Delta city clusters-their interactions and seasonal variation, *Theor Appl Climatol*, 103, 489-499,

894 | 10.1007/s00704-010-0323-6, 2011.

895 | Wu, K., and Yang, X. Q.: Urbanization and heterogeneous surface warming in eastern China, *Chinese Sci Bull*, 58,

896 | 1363-1373, 10.1007/s11434-012-5627-8, 2013.

897 | Xie, M., Zhu, K. G., Wang, T. J., Yang, H. M., Zhuang, B. L., Li, S., Li, M. G., Zhu, X. S., and Ouyang, Y.:

898 | Application of photochemical indicators to evaluate ozone nonlinear chemistry and pollution control

899 | countermeasure in China, *Atmos Environ*, 99, 466-473, 10.1016/j.atmosenv.2014.10.013, 2014.

900 | Xie, M., Zhu, K. G., Wang, T. J., Feng, W., Zhu, X. S., Chen, F., Ouyang, Y., Liu, Z. J.: Study on the distribution

901 | of anthropogenic heat flux over China, *China Environmental Science*, 35, 728-734, 2015.

902 | Xie, M., Liao, J., Wang, T., Zhu, K., Zhuang, B., Han, Y., Li, M., Li, S. -: Modeling of the anthropogenic heat

903 | flux and its effect on regional meteorology and air quality over the Yangtze River Delta region, China, *Atmos.*

904 | *Chem. Phys.*, 16, 6071-6089, 10.5194/acp-16-6071-2016, 2016.

905 | Yu, M., Carmichael, G. R., Zhu, T., and Cheng, Y. F.: Sensitivity of predicted pollutant levels to anthropogenic

906 | heat emissions in Beijing, *Atmos Environ*, 89, 169-178, 10.1016/j.atmosenv.2014.01.034, 2014.

907 | Zhang, D. L., Shou, Y. X., and Dickerson, R. R.: Upstream urbanization exacerbates urban heat island effects,

908 | *Geophys Res Lett*, 36, Artn L24401_

909 | 10.1029/2009gl041082, 2009a.

910 | Zhang, Q., Streets, D. G., Carmichael, G. R., He, K. B., Huo, H., Kannari, A., Klimont, Z., Park, I. S., Reddy, S.,

911 | Fu, J. S., Chen, D., Duan, L., Lei, Y., Wang, L. T., and Yao, Z. L.: Asian emissions in 2006 for the NASA

912 | INTEX-B mission, *Atmos Chem Phys*, 9, 5131-5153, 2009b.

913 | Zhang, Y. N., Xiang, Y. R., Chan, L. Y., Chan, C. Y., Sang, X. F., Wang, R., and Fu, H. X.: Procuring the regional

914 | urbanization and industrialization effect on ozone pollution in Pearl River Delta of Guangdong, China, *Atmos*

915 | *Environ*, 45, 4898-4906, 10.1016/j.atmosenv.2011.06.013, 2011.

916 | Zheng, J. Y., Zhang, L. J., Che, W. W., Zheng, Z. Y., and Yin, S. S.: A highly resolved temporal and spatial air

917 | pollutant emission inventory for the Pearl River Delta region, China and its uncertainty assessment, *Atmos*

918 | *Environ*, 43, 5112-5122, 10.1016/j.atmosenv.2009.04.060, 2009.

919 | Zhu, K., Blum, P., Ferguson, G., Balke, K. D., and Bayer, P.: The geothermal potential of urban heat islands,

920 | *Environ Res Lett*, 5, Artn 044002_

921 | 10.1088/1748-9326/5/4/044002, 2010.

922 | Zhu, B., Kang, H. Q., Zhu, T., Su, J. F., Hou, X. W., and Gao, J. H.: Impact of Shanghai urban land surface forcing

923 | on downstream city ozone chemistry, *J Geophys Res-Atmos*, 120, 4340-4351, 10.1002/2014JD022859, 2015.

924